A NUMERICAL MODELING OF THE ATMOSPHERIC
SELF-PRESERVING SIZE DISTRIBUTION

BY

FRANK W. BUEHNER
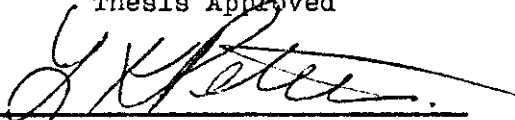
Advisor:  Dr. L. K. Peters

A Thesis Submitted to the
Department of Chemical Engineering of
The Cleveland State University
in partial fulfillment of the requirements
for the degree of
Master of Science
June, 1973

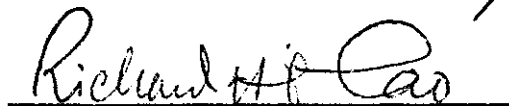A NUMERICAL MODELING OF THE ATMOSPHERIC

SELF-PRESERVING SIZE DISTRIBUTION

.

BY

FRANK W. BUEHNER

Thesis Approved

Thesis Advisor

# PREFACE

The coagulation equation had previously been studied with a feed term, but no settling term. This was probably due to the fact that the resulting equation contained two independent variables and its computer solution required unreasonable amounts of time.

An apparent steady state size distribution of aerosol particles in the atmosphere was known to exist and had been measured at various locations. This prompted a steady state solution to the coagulation equation with both feed and settling terms, but only one independent variable since the transient term would be ignored.

I am grateful to the help given me by my thesis advisor, Dr. Leonard K. Peters, who was always willing to help when insurmountable problems arose. His interest in the results of this work was a constant incentive when my productivity waned.

Several people aided me in gaining the unusually large amount of computer time necessary for the completion of this work. The first is Mrs. Susan Wilson who was in charge of large core scheduling. The second is Mrs. Ingrid Flower who was an administrative specialist in the data control department.

I must acknowledge my father, Mr. Henry Buehner, who provided me with funds and the use of his Florida home during the initial draft of this work and Miss. Katalin Gaal, who provided a sanctum during the typing of the final copy.

Final thanks go to the chemical engineering department and the Lubrizol Corporation who extended financial support during my graduate studies.

The total computer time necessary for completion of this work was 127 hours task time and 201 hours real time.

This work is dedicated to my mother, Mrs. Henry Buehner.

## ABSTRACT

The dynamics of polydisperse aerosol systems is described by the following equations for each particle size j:

$$\partial n_j/\partial t = F_j + 2\pi \sum_{\substack{i=1 \\ m=j-i}}^{k=j-1} D_{i,m} R_{i,m} n_i n_m \;-\; 4\pi n_j \sum_{m=1}^{k} D_{j,m} R_{j,m} n_m$$

$$-\; \bar{v}_j \partial n_j/\partial y.$$

Hidy ( 7 ) has numerically investigated the transient system when the feed( $F_j$ ) and sedimentation( $\bar{v}_j \partial n_j/\partial y$ ) terms were neglected. Later, Mockros et al. ( 10 ) included the feed term in their analysis of the unsteady state system. Both investigations were looking for asymptotic behavior in connection with the self-preserving size distribution of the atmospheric aerosol. However, neglecting the settling term inherently restricted their results to the upper end of the size spectrum which contains the smaller particles.

This study investigates the concept of the self-preserving size distribution by including the settling term, feed term, and coagulation terms, but ignoring the transient. Thus, the asymptotic behavior of the dynamic steady state is obtained. Various feed configurations are studied with respect to the steady state size distribution as regards similarities to the self-preserving size distribution in the atmosphere.

A system containing 400 discrete size classes is solved using a fourth-order Runge-Kutta integration routine to integrate in distance.

Results indicate that the solution to the steady state equation in self-preserving form is dependent upon both the feed concentration and distribution. A definite similarity to experimental

evidence for the atmospheric self-preserving size distribution is seen when the dimensionless particle concentrations are plotted in the proper form.

TABLE OF CONTENTS

# LIST OF TABLES

# LIST OF FIGURES

# INTRODUCTION

Dispersed systems with a gas-phase medium and a solid or liquid disperse phase are called aerosols or aerodisperse systems. Until recently, no rational classification was used to differentiate between aerosols formed by dispersion and condensation while distinguishing systems having solid or liquid disperse phases.

Today there exists a scientific classification of aerosols which coincides with everyday non-technical language. Condensation and dispersion aerosols with liquid particles are called mists, regardless of particle size. Dispersion aerosols with solid particles are called dusts, again regardless of particle size. Finally, condensation aerosols with a solid phase are called smokes; these include systems of condensation origin containing both liquid and solid particles. ( Figure 1)

The subject of atmospheric particulates involves sizes in the very wide range of $10^{-7}$ to $10^{-1}$ cm. Passage from the lower to the upper limit in particle size is accompanied by changes not only in many of the physical properties, but also in the nature of the laws governing them. This can be seen particularly clearly in the resistance which a gas offers to the motion of particles. For very small particles ( $r < 10^{-6}$ cm. ) the resistance is proportional to the velocity and the square of the particle radius. In the range $10^{-6}$ to $10^{-4}$ cm. there is a gradual change to Stokes Law; the resistance remains proportional to the velocity, but the dependence upon radius becomes linear. Further increase in radius brings deviation from Stokes Law in the opposite direction; for velocities that are not very low the proportionality of resistance and velocity ceases, while at sufficiently large velocities and particle sizes, the resistance is more nearly proportional to the square of the radius and the square of the velocity( 5 ). ( Figure 2 )

When particles become sufficiently small( $r \sim .2 \mu$ ), Brownian motion becomes important. This type of motion is caused by an uneven

AEROSOL

| | | | | | |
|---|---|---|---|---|---|
| Mist | Fog | | | Tobacco Smoke | |
| Ground Stone | $H_2SO_4$ Concentrator Mist | | Rosin | Smoke | |
| | | $SO_3$ Mist | Carbon Black | | |
| Spray Dried Detergent | | Pigments | | | |
| | | $NH_4Cl$ Fume | | | Molecular Radii |
| | Pulverized Coal | Spray Dried Milk | Oil Smoke | | |
| Stoker Fly Ash | | | | Colloidal Rocket | |
| | Fly Ash | | | | |
| Foundry Dusts | | Zinc Oxide Fume | | | |
| | Cement Dust | Alkali Fume | | | |
| | | MgO Smoke | | | |
| | Metallurgical Dust | | | | |
| | | Metallurgical Fume | | | |
| Pollens | | Bacteria | Virus | Protein | |
| | | Metallic Debri in Rockets | | | |
| Household and Agricultural Sprays | | | | | |
| Meteorites | | | | | |

GAS CLEANING DEVICES

| | | | | |
|---|---|---|---|---|
| Settling Chamber | | | | |
| Impingers and Impacters | | | | |
| Centrifugal | Dust Separaters (Cyclones) | | | |
| Centrifuges | | | | |
| Bag-House Filters | | | | |
| Sonic Agglomerators | | | | |
| Electrostatic Precipitators | | | | |
| Thermal Precipitators | | | | |
| Millipore and Similar Filters | | | | |

1000 $\mu$    100 $\mu$    10 $\mu$    $R_i$    1 $\mu$    $10^{-1}\mu$    $10^{-2}\mu$    $10^{-3}\mu$

Figure 1. Some Common Aerosols and Gas Cleaning Devices (5)
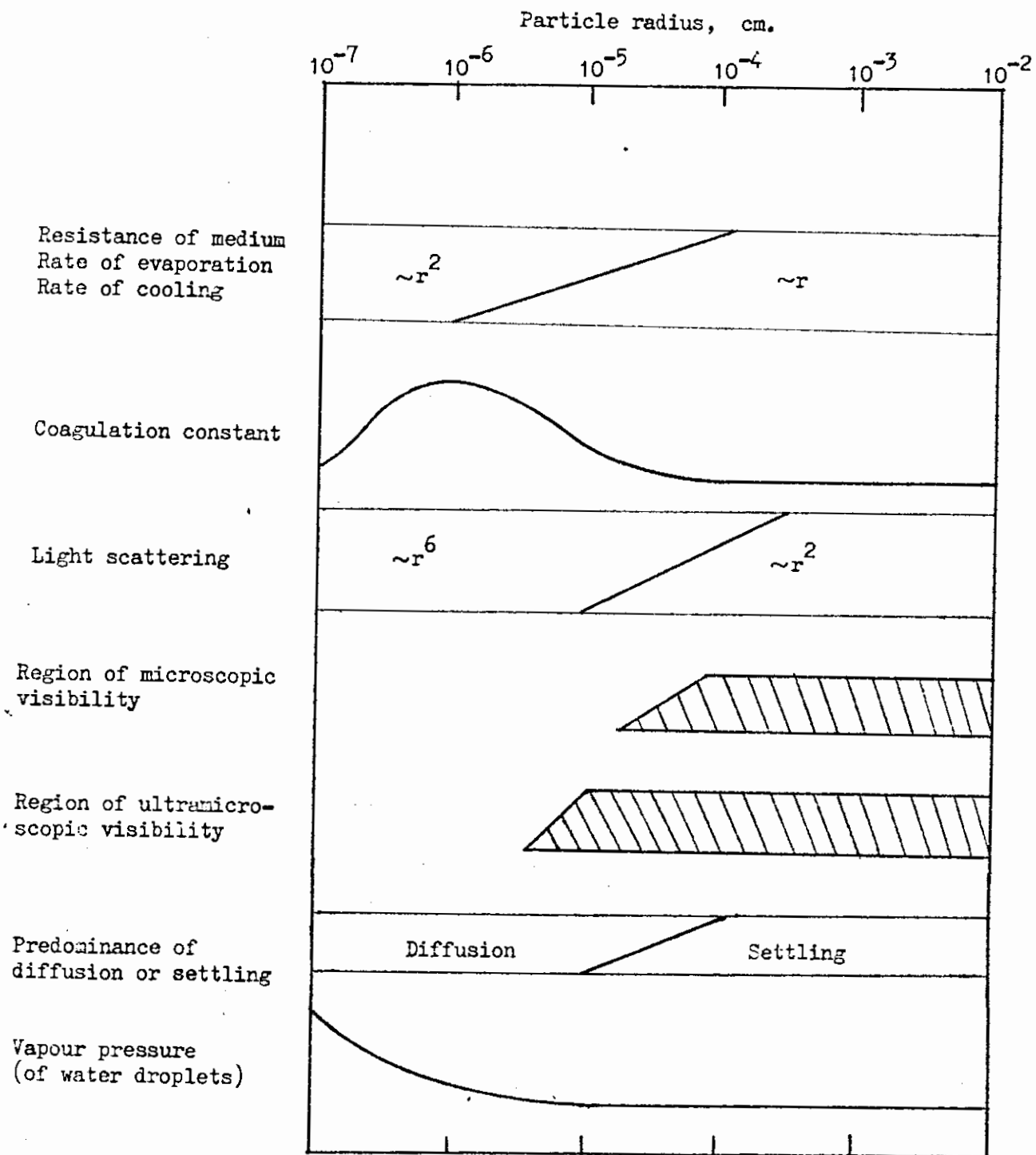
Figure 2. Some Properties of Aerosols in Relation to Particle Size ( 5 )

bombardment of the particles by the fluid molecules. There are
fluctuations in the net force resulting in the particles following
a circuitous path. However, the particle mass is so large compared
to that of the fluid molecules that changes in direction of the
particle are not present until a large number of collisions with
fluid molecules have occurred.

When aerosol particles come into contact and coalesce or
adhere to one-another the process is called coagulation. Particles
may come into proximity because of their Brownian motion, resulting
in thermal coagulation. Superimposed on this there may be an orderly
motion produced by hydrodynamic, electrical, gravitational or other
forces. The velocity of approach due to such forces may be large
enough to set up a rate of coagulation that is large compared with
that due to Brownian motion. Thermal coagulation is spontaneous,
as is the coagulation of aerosols containing charged particles.
Other cases are frequently referred to as forced coagulation.

The atmosphere is a mixture of man-made and natural aerosols
which is continuously fed by industrial and municipal smokes,
volcanic dusts, water vapor, later to become mist, and particu-
lates from a myriad of other sources. The atmosphere, however,
does not retain all these particles. Losses are accomplished by
coagulation of the aerosols to ever increasing particle radii until
they settle by gravity. Other mechanisms such as washout by rain
are also active.

Various investigaters have found a size distribution with a
shape that is apparently universal to urban and suburban areas.
The only apparent differences are vertical shifts in the curve due
to absolute number density( Figure 3 ). This size distribution is
similar to the decay of turbulent energy of fluids in pipes. In
fact, similarity transforms based on turbulent energy transfer
analogies have been used to study coagulation equations since they
cannot be solved explicitly ( 16 ).
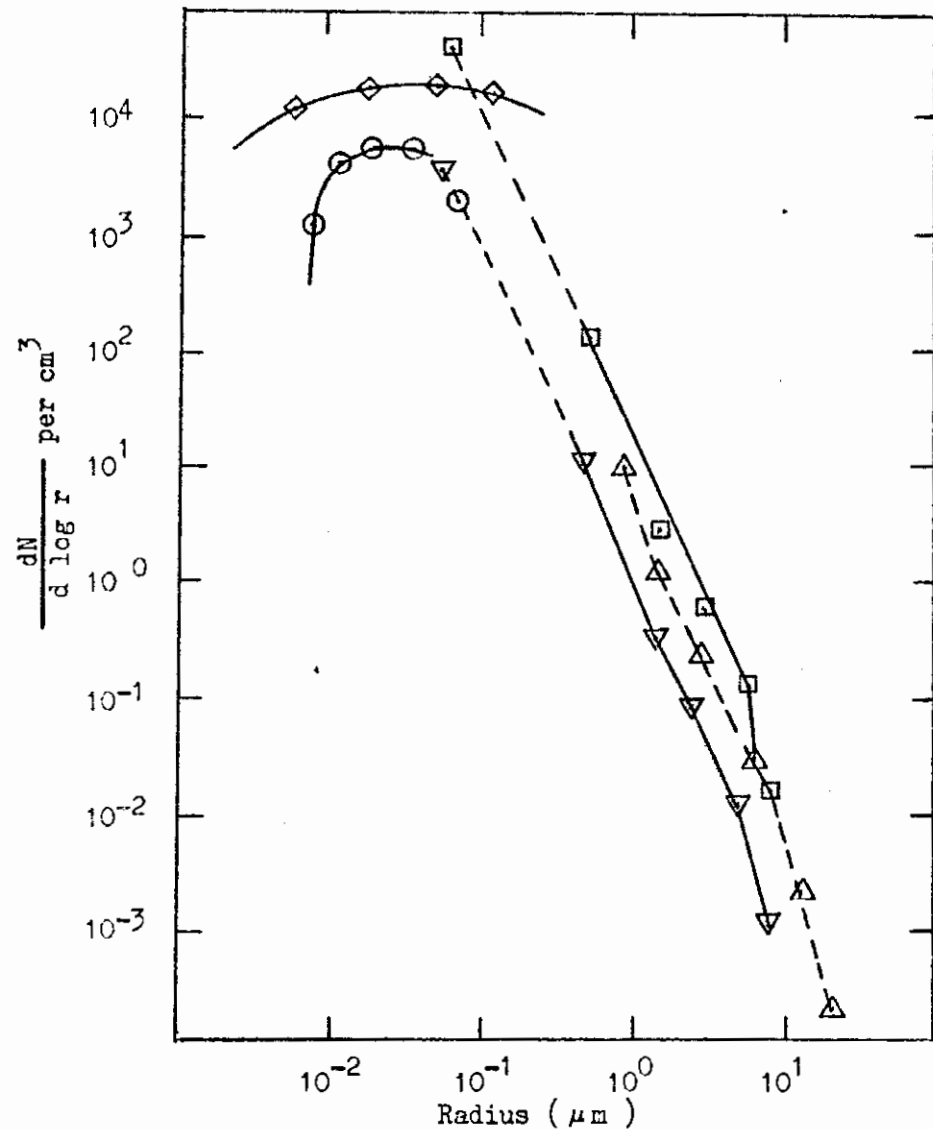
Figure 3. Complete Size Distributions of Aerosols at Various
Locations in Germany. Individual curves are based on average data
of many measurements and are not based entirely on simultaneous
sampling. The dashed curves between $8 \times 10^{-2}$ and $4 \times 10^{-1}$ $\mu$m are
interpolated. The points $\diamond$ and $\odot$ are based on ion mobility meas-
urements at Frankfurt and the Zugspitze, respectively. Other
points are based on impactor measurements or nuclei count:$\nabla$ Zugspitze;
$\square$ Frankfurt; $\triangle$ Zugspitze sedimentation data. ( 15 )

Various investigators have solved the coagulation equation numerically for monodisperse and polydisperse aerosol systems (7,19), but none have solved it including both feed and sedimentation terms. The reason for this becomes obvious when it is noted that this would involve simultaneous solution in two independent variables for large numbers of particle sizes. The numerical solution of the coagulation equation with one independent variable presses today's computers to their limit and two would be unwieldy.

It was decided, therefore, to solve the steady state case of the coagulation equation with feed and settling terms having the goal of numerically simulating the experimental evidence found for the apparent steady state size distribution in the atmosphere( the atmospheric self-preserving size distribution).

Since the shape of the atmospheric distribution was seen to be retained at various locations and altitudes, it was hypothesized that the feed term could take on widely varying forms and yet yield a shape reasonably consistent with that observed.

Aknowledged at the start of this work was the fact that the complete numerical simulation of the steady state atmospheric distribution would require more computer time and data storage area than would be feasible. Therefore, it was decided to calculate solutions for three sections of the curve and attempt to fit them together employing various curve smoothing techniques if necessary.

CHAPTER II

LITERATURE SURVEY

Investigations of the coagulation equation have accelerated in the
last few years. The increase in air pollution concern and investigators
quest for an understanding of the mechanics of aerocolloidal systems are
partly responsible for this increased interest.

The first coagulation model was developed by Smoluchowski (13) who
developed expressions for a discrete or discontinuous distribution of
particle concentrations in various sizes (the size spectrum). Particles
of a particular size were considered as aggregates consisting of j mult-
iples of a unit size. The relation for the growth rate of a sol was then
given by a set of nonlinear differential equations expressing the change
in concentration with time of each j-sized aggregate.

Hidy (7) numerically investigated a form of Smoluchowski's equation
with a slip correction for the Brownian diffusion coefficient. This
study employed various initial concentrations and $\lambda/r_1^*$, the particle
size parameter. Hidy found that the discrete size spectrum approached a
self-preserving form after a sufficiently large dimensionless coagula-
tion time. However, his solutions were limited to the upper section of
the spectrum because of the lack of a settling term in his work.

Mockros, et al. (10) investigated a form of Smoluchowski's equation
modified to include a feed term. They concluded that the largest con-
centration occured at the particle size associated with the highest rate
of input and the peak size was invarient with time.

Friedlander and Wang (4) studied a continuous form of the coagula-
tion equation with a constant collision frequency factor. This study
concluded that the self-preserving spectrum was greatly influenced by
the form of the collision frequency factor, particularly the lower end.

Other evidence supporting the hypothesis that the self-preserving
size spectra are asymptotic forms approached by coagulating dispersions

---

* See NOMENCLATURE for a complete listing of symbols

was found by Swift and Friedlander (16) whose coagulating oil-in-water emulsion experiments were found to be self-preserving in form.

Since various investigations of the coagulation equation employing similarity transforms supported the hypothesis of a self-preserving size spectrum, a direct solution of the coagulation equation was in order. This would involve the addition of a feed and settling term to the basic coagulation equation in order to more realistically simulate the atmospheric aerosol. Also, since Friedlander and Wang (4) found that a constant collision frequency factor influenced their results, the variable factor would be used.

# CHAPTER III

## THEORETICAL ANALYSIS

### Basic Assumptions and Derivation of Particle "types"

Attempting a mathematical description of a polydisperse aerosol system with feed and sedimentation, one proceeds from the development of a polydisperse coagulation equation to an elemental particle balance on the system. The dynamic steady state behavior is then obtained by including the settling, feed, and coagulation terms but ignoring the transient.

Theories of Brownian, or thermal, coagulation usually start with the assumption that particles adhere at every collision. Except for large particles this assumption has firm theoretical and experimental basis ( 5 ). They also presume that all collisions yield perfect spheres, that there are only binary collisions, and that the dispersing medium is static with no electrostatic charges present.

If a particle "type" related to the radius is established with the smallest particle in the system designated as particle "type 1" then it is possible to relate a discrete system of particles by their "type". For example, a "type 3" particle may have been fed in or formed by the coagulation of a "type 2" and a "type 1" particle ("types" are additive). The "type 3" particle can be related by it's radius to the "type 1" particle by the relation

$$r_3 = r_1\sqrt[3]{3}.$$

( III-1)

The following relations follow

$$r_4 = r_1\sqrt[3]{4}$$

( III-2)

$$r_5 = r_1 \sqrt[3]{5} \quad \text{etc.} \qquad\qquad ( \text{III-3} )$$

These relations can be recognized as follows: In a discrete system the volume of all particles must be multiples of the volume of particles of radius $r_1$. Since mass must be conserved, the collision between two $r_1$ particles yield a particle $r_2$ of mass

$$2( \frac{4}{3} \pi r_1^3 \rho ) = ( \frac{4}{3} \pi r_2^3 \rho ) \qquad\qquad ( \text{III-4} )$$

or

$$r_2 = r_1 \sqrt[3]{2}. \qquad\qquad ( \text{III-5} )$$

In general, the following relationship holds

$$r_j = r_1 \sqrt[3]{j}. \qquad\qquad ( \text{III-6} )$$

Derivation of the Coagulation Equation

In analogy to chemical kinetics, the following coagulation reaction occurs

$$2 \text{ "type 1" particles} \xrightarrow{\text{K}_{1,1}} 1 \text{ "type 2" particle.} \qquad ( \text{III-7} )$$
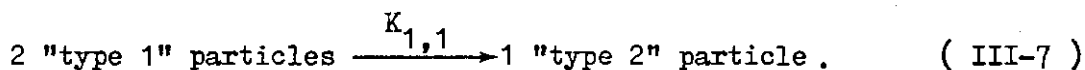
Thus, the disappearance of "type 1" particles according to Equation ( III-7 ) is

$$- \frac{dn_1}{dt} = 2 K_{1,1} n_1^2 \qquad ( \text{III-8} )$$

and the appearance of "type 2" particles according to Equation ( III-7 ) is

$$\frac{dn_2}{dt} = K_{1,1} n_1^2 \qquad ( \text{III-9} )$$

where subscripts denote particle "types" and

$n$ = concentration of particles

$\dfrac{dn_1}{dt}$ = rate of change of the particle concentration due to coagulation

$K_{1,1}$ = coagulation constant for the process described .

The 2 appears in Equation ( III-8 ) because there are two "type 1" particles lost from the "type 1" size class when a "type 2" particle is formed.

"Type 1" particles disappear not only because of collisions with other "type 1" particles, but also due to collisions with "type 2", "type 3", etc. , aggregates with the following always applying

$$-\left(\frac{dn_1}{dt}\right)_{1,2} = K_{1,2}n_1n_2 \qquad (\text{ III-10 })$$

or in general

$$-\left(\frac{dn_1}{dt}\right)_{1,k} = K_{1,k}n_1n_k. \qquad (\text{ III-11 })$$
$$k \neq 1$$

Altogether, the following then applies for the disappearance of "type 1" particles

$$-\left(\frac{dn_1}{dt}\right) = 2K_{1,1}n_1^2 + K_{1,2}n_1n_2 + \ldots + K_{1,k}n_1n_k. \quad (\text{ III-12 })$$

If the entire coagulation process is to be described, the change with time of the total number of all particles must be calculated. This temporal change is

$$\frac{d}{dt}\sum_{j=1}^{k} n_j = \frac{dn_1}{dt} + \frac{dn_2}{dt} + \ldots + \frac{dn_k}{dt}. \quad (\text{ III-13 })$$

It is necessary, therefore, to calculate the terms

$$\frac{dn_2}{dt} \quad , \quad \frac{dn_3}{dt} \quad , \quad etc.$$

As in Equation ( III-12 ), the loss of "type 2" aggregates by coagulation is

$$-\left(\frac{dn_2}{dt}\right)_L = K_{2,1}n_2n_1 + 2K_{2,2}n_2^2 + K_{2,3}n_2n_3 + \ldots$$

$$+ K_{2,k}n_2n_k \qquad\qquad ( III-14 )$$

where the subscript L designates loss.

In short

$$-\left(\frac{dn_2}{dt}\right)_L = n_2\sum_{m=1}^{k} K_{2,m}n_m + K_{2,2}n_2^2 . \qquad ( III-15 )$$

However, during the same period of time an increase of "type 2" particles occurs due to the coagulation of "type 1" particles. As two "type 1" particles are needed to form a "type 2" particle, this increase according to Equation ( III-9 ) is

$$+\left(\frac{dn_2}{dt}\right)_G = K_{1,1}n_1^2 \qquad\qquad ( III-16 )$$

where the subscript G designates gain.

The net change of "type 2" particles is thus given by the use of Equations ( III-15 ) and ( III-16 );

$$-\left(\frac{dn_2}{dt}\right)_{L+G} = n_2 \sum_{m=1}^{k} K_{2,m} n_m + K_{2,2} n_2^2 -$$

$$K_{1,1} n_1^2 . \qquad\qquad ( \text{III-17} )$$

The coagulation-conditioned decrease of the larger aggregates is subject to the formal structure of Equation ( III-14 ) or ( III-15 ). If in Equation ( III-15 ), the specific subscript "2" is replaced by the general subscript "j", we obtain

$$-\left(\frac{dn_j}{dt}\right)_{L} = n_j \sum_{m=1}^{k} K_{j,m} n_m + K_{j,j} n_j^2 \qquad ( \text{III-18} )$$

The format of the type of aggregate observed at any particular time may follow several processes starting from "type 4" aggregates. Since formation of aggregates by three or more simultaneous collisions has been excluded by assumption, "type 4" particles can be created by two "type 2" particles or by a "type 3" and a "type 1" particle. For the generation of "type 3" aggregates we thus have

$$+\left(\frac{dn_3}{dt}\right)_{G} = K_{1,2} n_1 n_2 \qquad\qquad ( \text{III-19} )$$

and for "type 4" aggregates

$$+\left(\frac{dn_4}{dt}\right)_G = K_{2,2}n_2^2 + K_{1,3}n_1n_3. \qquad (\text{III-20})$$

The last expression can be written in generalized form as[*]

$$+\left(\frac{dn_j}{dt}\right)_G = \frac{1}{2}\sum_{\substack{i=1\\m=j-i}}^{k=j-1} K_{i,m}n_in_m + \left[\begin{array}{c}\frac{1}{2}K_{j/2,j/2}n_{j/2}^2\\ \\ \text{for j even}\end{array}\right]. \qquad (\text{III-21})$$

If the two components of the coagulation process, i.e. , Equations ( III-18 ) and ( III-21 ) are combined, the following equation for the net change with time of the number of specific multiple aggregates consisting of j "type 1" particles is obtained;

$$-\left(\frac{dn_j}{dt}\right)_{L+G} = n_j\sum_{m=1}^{k} K_{j,m}n_m + K_{j,j}n_j^2 - \qquad (\text{III-22})$$

$$\frac{1}{2}\sum_{\substack{i=1\\m=j-i}}^{k=j-i} K_{i,m}n_in_m - \left[\begin{array}{c}\frac{1}{2}K_{j/2,j/2}n_{j/2}^2\\ \\ \text{for j even}\end{array}\right].$$

---

[*] $K_{i,j}$ is equivalent to $K_{j,i}$

When the total is summed over j, the net change, with time, of the total particle number is obtained ( this describes the overall coagulation process).

Two terms appear in the coagulation equation which do not appear in summations, namely

$$+ \ K_{j,j}n_j^2 \qquad\qquad ( \text{III-23} )$$

and

$$- \left[ \frac{1}{2} K_{j/2,j/2}n_{j/2}^2 \quad \text{for j even} \right]. \qquad ( \text{III-24} )$$

These are normally assumed to be negligible when compared to the summation terms. In this work they were shown to be negligible (See Apendix A ) by a trial computer program comparison. Qualitatively, these two terms can also be shown to be negligible. Since they represent single terms compared with summations that can have many terms, their significance is decreased by the summations. Also, coagulation constants bearing like subscripts, i.e., those representing probabilities of collisions between like sized particles, are much smaller than probabilities of collisions between unlike sized particles ( Table 1 ). Hence, the coagulation equation is simplified to

$$- \left( \frac{dn_j}{dt} \right)_{L+G} = n_j \sum_{m=1}^{k} K_{j,m}n_m - \frac{1}{2}\sum_{\substack{i=1 \\ m=j-i}}^{k=j-1} K_{i,m}n_i n_m. \qquad ( \text{III-25} )$$

| $r_1$ (cm.) \ $r_2$ (cm.) | $10^{-7}$ | $2 \times 10^{-7}$ | $5 \times 10^{-7}$ | $10^{-6}$ | $2 \times 10^{-6}$ | $5 \times 10^{-6}$ | $10^{-5}$ | $2 \times 10^{-5}$ | $5 \times 10^{-5}$ | $10^{-4}$ | $2 \times 10^{-4}$ | $5 \times 10^{-4}$ | $10^{-3}$ |
|---|---|---|---|---|---|---|---|---|---|---|---|---|---|
| $10^{-7}$ | 4.5 | | | | | | | | | | | | |
| $2 \times 10^{-7}$ | 7.5 | 6 | | | | | | | | | | | |
| $5 \times 10^{-7}$ | 30 | 13 | 9 | | | | | | | | | | |
| $10^{-6}$ | 90 | 40 | 15 | 12 | | | | | | | | | |
| $2 \times 10^{-6}$ | 300 | 110 | 35 | 17 | 11 | | | | | | | | |
| $5 \times 10^{-6}$ | 1600 | 550 | 120 | 40 | 15 | 7.2 | | | | | | | |
| $10^{-5}$ | $5 \times 10^3$ | 1400 | 270 | 80 | 25 | 8 | 5.2 | | | | | | |
| $2 \times 10^{-5}$ | $13 \times 10^3$ | 4100 | 660 | 170 | 47 | 11 | 5.3 | 4.0 | | | | | |
| $5 \times 10^{-5}$ | $37 \times 10^3$ | 9500 | 1600 | 420 | 115 | 24 | 9 | 4.7 | 3.4 | | | | |
| $10^{-4}$ | $77 \times 10^3$ | $20 \times 10^3$ | 3200 | 840 | 230 | 45 | 16 | 7.1 | 3.7 | 3.2 | | | |
| $2 \times 10^{-4}$ | $160 \times 10^3$ | $40 \times 10^3$ | 6600 | 1700 | 450 | 90 | 30 | 12 | 5.2 | 3.5 | 3.0 | | |
| $5 \times 10^{-4}$ | $400 \times 10^3$ | $100 \times 10^3$ | $16 \times 10^3$ | 4300 | 1100 | 220 | 72 | 28 | 10.3 | 5.6 | 3.7 | 3.0 | |
| $10^{-3}$ | $800 \times 10^3$ | $200 \times 10^3$ | $30 \times 10^3$ | 8500 | 2200 | 430 | 140 | 54 | 19 | 9.6 | 5.5 | 3.3 | 3.0 |

$$K(r_1, r_2) \cdot 10^{10} \quad (\text{cm.}^3 \text{ sec.}^{-1})$$

Table 1. Coagulation Constants for Unequal Particles ( 5 )

## Derivation of the Coagulation Constant

The coagulation constant described by Equation ( III-7 ) is, in actuality, a probability of collision between two dispersed particles as a result of their Brownian motion. The coagulation constant is most easily derived by taking advantage of the similarity between Brownian motion and diffusion. The model assumes a single stationary spherical particle with a radius $r_i$ and a diffusing particle of radius $r_j$. In the range of particle sizes considered here, Van der Waals forces strongly attract particles that come into close proximity by way of their Brownian motion and are bonded together. This means that over a spherical surface of radius $r_i + r_j$ , the particle concentration remains zero. The diffusional flux across the surface depends on the average rate at which particles cross as a result of their Brownian motion.

In order to find the diffusional flux, the distribution of particles diffusing toward the sphere of radius $r_i$ is considered in spherical coordinates with angular and azimuthal symmetry. The concentration, n, of these particles satisfies the unsteady state diffusion equation;

$$\frac{\partial n_j}{\partial t} = D \frac{1}{r^2} \frac{\partial}{\partial r} \left( r^2 \frac{\partial n_j}{\partial r} \right) \qquad ( III-26 )$$

where D is the Brownian diffusion coefficient of the aerosol particles.

The system is shown in Figure 4. The boundary and initial conditions for a diffusing polydisperse aerosol are
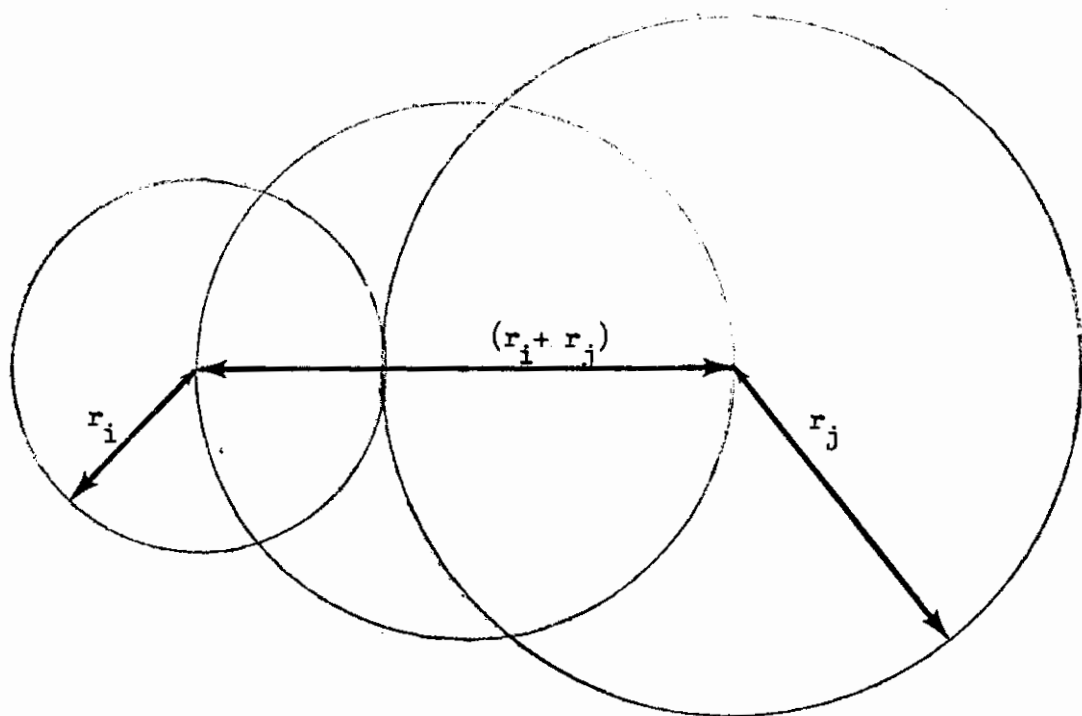
Figure 4. The Coagulation Diffusion Model

i) $t = 0$, $r > r_i + r_j$ , $n_j = n_{j0}$

ii) $t > 0$, $r \longrightarrow \infty$ , $n_j = n_{j0}$      ( III-27 )

iii) $t > 0$, $r = r_i + r_j$ , $n_j = 0$

The first boundary condition states that the initial concentration of "type j" particles is a constant with the initial distance between particles greater than the coagulation radius, $r_i + r_j$ . The second boundary condition is for an infinite medium, while the third is for the assumption that each collision is effective. The final form is presented by various authors ( 5, 7, 16 ) and is based on the solution of the appropriate stochastic problem by A. N. Kolmogorov and M. A. Leontovich ( 8 ). For the sake of brevity, the solution is

$$\frac{n_j}{n_{j0}} = 1 - \frac{r_i + r_j}{r} + \mathrm{erf}\left[\frac{r - ( r_i + r_j )}{2\sqrt{Dt}}\right] \qquad ( \text{III-28} )$$

where

$$\mathrm{erf}\,\xi = \frac{2}{\sqrt{\pi}}\int_0^{\xi} e^{-\delta^2} d\delta.$$

The flux toward the particle is

$$- j^*\Big|_{r_i + r_j} = -\left(- D\frac{\partial n_j}{\partial r}\right)\Big|_{r = r_i + r_j}. \qquad ( \text{III-29} )$$

When Equation ( III-28 ) is operated on by Equation ( III-29 ) the result is

$$\frac{\partial n_j}{\partial r} = n_{j0} \left[ \frac{r_i + r_j}{r^2} + \frac{e^{-\left\{\frac{r - (r_i + r_j)}{2\sqrt{Dt}}\right\}^2}}{\sqrt{\pi Dt}} \right] \quad ( \text{ III-30 } )$$

and

$$D \left( \frac{\partial n_j}{\partial r} \right)\Bigg|_{r = r_i + r_j} = \frac{Dn_{jo}}{r_i + r_j} \left[ 1 + \frac{r_i + r_j}{\sqrt{\pi Dt}} \right].\quad ( \text{ III-31 } )$$

Thus, the number of j particle contacts per i particle per unit time is

$$\sigma_{i,j} = \int_{s^*} - j^* \, ds^* = \frac{Dn_{j0}}{r_i + r_j} \left( 1 + \frac{r_i + r_j}{\sqrt{\pi Dt}} \right) \times$$

$$\left\{ 4\pi \, (\, r_i + r_j \,)^2 \right\} \quad ( \text{ III-32 } )$$

or

$$\sigma_{i,j} = 4\pi D n_{j0} \, (\, r_i + r_j \,) \left( 1 + \frac{r_i + r_j}{\sqrt{\pi Dt}} \right) \quad ( \text{ III-33 } )$$

where $s^*$ = surface area of coagulation radius.

It is now assumed that the coagulation process is viewed t seconds after its start, when $t \gg ( r_i + r_j )^2 / D$ . In the case of usual particle dimensions this means that the elapsed start of the coagulation process exceeds $10^{-3}$ to $10^{-4}$ seconds ( 1 ). The number of encounters of i particles by j particles per unit time after this initial period is then

$$\sigma_{i,j} = 4\pi D n_{j0} ( r_i + r_j ). \qquad ( \text{III-34} )$$

An advance will now be made from the idea of a stationary absorbing sphere in order to account for the arbitrary movement of both particles. Suppose that i and j particles move in space, respectively, a distance $\Delta X_i$ and $\Delta X_j$ in a time interval $\Delta t$. Then their relative square displacement on the average is

$$\overline{( \Delta X_i - \Delta X_j )^2} = \overline{\Delta X_i^2} + \overline{\Delta X_j^2} - 2 \overline{\Delta X_i \Delta X_j}. \qquad ( \text{III-35} )$$

Since $\Delta X_i$ and $\Delta X_j$ are independent

$$\overline{\Delta X_i \Delta X_j} = 0 \qquad ( \text{III-36} )$$

and

$$\overline{( \Delta X_i - \Delta X_j )^2} = \overline{\Delta X_i^2} + \overline{\Delta X_j^2}. \qquad ( \text{III-37} )$$

Hence, with the use of Einstein's expression for the diffusivity
( 5 ), the corrected diffusivity for this case becomes

$$\overline{x^2} = \overline{( \Delta X_i - \Delta X_j )^2} = 2D\Delta t = 2 ( D_i + D_j )\Delta t. \qquad ( III-38 )$$

Therefore

$$D = D_i + D_j \qquad ( III-39 )$$

and

$$\sigma_{i,j} = 4\pi n_{j0} ( D_i + D_j )( r_i + r_j ). \qquad ( III-40 )$$

Now, the total number of j particle contacts per unit time is
( see Equation ( III-34 ))

$$J_{i,j} = \sigma_{i,j} n_{i0}$$

$$= 4\pi ( D_i + D_j )( r_i + r_j )n_{i0}n_{j0}. \qquad ( III-41 )$$

Since all collisions are assumed effective, $J_{i,j}$ represents the rate
of formation of multiple particles by the coagulation of particles of
"type i" and "type j".

Because time is assumed much greater than the ratio of the
square of the coagulation radius ( $r_i + r_j$ ) to the particle diff-
usivity ( D ), the collision frequency, $J_{i,j}$ , does not depend ex-
plicitly on time. The collision frequency between particles of size
i and j is proportional to the concentration of each multiple pres-
ent. By this reasoning, the subscript 0 appearing in the concentration

terms in Equation ( III-41 ) will be dropped at this point with the understanding that the terms $n_i$ and $n_j$ represent bulk phase concentrations. We thus have

$$J_{i,j} = 4\pi( D_i + D_j )( r_i + r_j ) n_i n_j. \qquad ( \text{III-42} )$$

Since the coagulation process can be represented as (see Equation-III-7 )

$$n_i + n_j \xrightarrow{\quad K_{i,j} \quad} n_{i+j} . \qquad ( \text{III-43} )$$

it follows, from Equation ( III-42 ) that

$$K_{i,j} = 4\pi D_{i,j} R_{i,j} \qquad ( \text{III-44} )$$

where

$$D_{i,j} = D_i + D_j \qquad ( \text{III-45} )$$

$$R_{i,j} = r_i + r_j. \qquad ( \text{III-46} )$$

$K_{i,j}$ is called the coagulation constant; it represents the probability of collisions between particles of radius $r_i$ and $r_j$ with bulk phase concentrations $n_i$ and $n_j$, respectively.

Equation ( III-44 ) can now be substituted into Equation ( III-25 ) to yield

$$-\left(\frac{dn_j}{dt}\right) = 4\pi n_j \sum_{m=1}^{k} D_{j,m} R_{j,m} n_m \;-\; 2\pi \sum_{\substack{i=1 \\ m=j-i}}^{k=j-1} D_{i,m} R_{i,m} n_i n_m \qquad (\text{III-47})$$

which is the equation describing the coagulation process of each particle type in a polydisperse aerosol system.

## The Stokes-Cunningham Correction

When particles suspended in a gas are nearly the same size as the mean free path of the gas $(\lambda)$, the resistance to their motion decreases. This causes an increase in the frequency of particle collisions and subsequently this should result in an increase in coagulation rate. This phenomenon is linked to the slip of gas at the surface of the particle. The "slippage" of gas along a surface is inherently a non-continuum effect; thus its theoretical analysis involves conditions where the parameter $\lambda/r_i$ is non-zero.

The correction developed by Cunningham used for the Stokes settling velocity and the Brownian diffusion coefficient for particles on the same size as the mean free path of the medium is

$$G' = G \left( 1 + A_i \frac{\lambda}{r_i} \right) \qquad ( \text{ III-48 } )$$

where

G = uncorrected value such as Stokes settling velocity

G' = corrected value.

$A_i$ is given by Davies ( 3 ) as

$$A_i = 1.257 + .400 e^{-( 1.10 \, r_i / \lambda )}. \qquad ( \text{ III-49 } )$$

Equation ( III-49 ) is valid for paticles falling in the approximate

size range $.25 \leq \dfrac{\lambda}{r_i} \leq 10.0$ . For this study Equation ( III-49 )

has been extended to $\dfrac{\lambda}{r_i} = 0.10$ .

## The Atmospheric Particle Balance

Equation ( III-47 ) is examined by various authors ( 4,6,7 ) with initial distributions that are either monodisperse or polydisperse. The form of Equation ( III-47 ) limits it to systems that are closed, i.e., those which have no input of particles to the system or loss of particles by sedimentation. This is physically unrealistic since a closed system will eventually become free of aerosol particles by sedimentation and/or adhesion to the walls of the vessel in which it is enclosed.

Equation ( III-47 ) can be modified to include feed and sedimentation terms in order to more realistically investigate the atmospheric aerosol which has numerous sources of particles. This is accomplished by performing a particle balance on an elemental volume of the atmosphere. The elemental volume is visualized ( see Figure 5 ) with sides dx, dy, and dz. Positive directions are indicated by the arrows. The force of gravity is in the same direction as y. Additional terms necessary for the elemental particle balance are

$F_j$ , the j particles as feed to the element

$\bar{v}_j$ , the Stokes terminal settling velocity of particles of radius j  ( "type j" )

and

$dV$ , the volume of the element, dx dy dz .

The balance becomes

( generation of j particles/sec. ) + ( j particles/sec. )$_{in}$

- ( j particles/sec. )$_{out}$ = ( accumulation of j particles )

( III-50 )

where
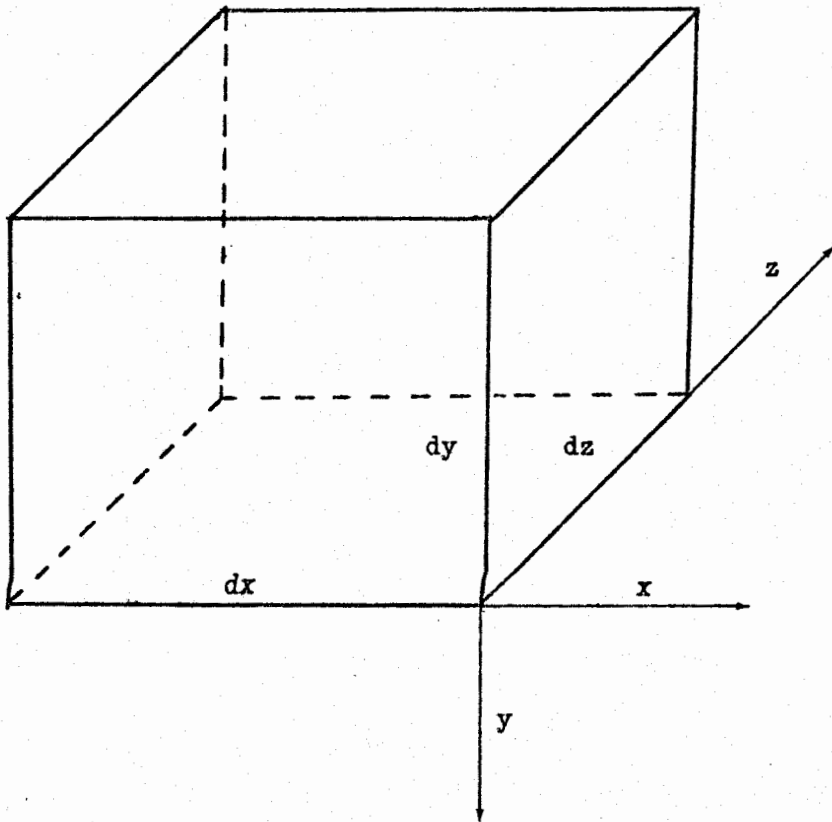
Figure 5. Elemental Volume of the Atmosphere

( generation of j particles/sec. ) = dV( change due to coagulation)

$$( \text{III-51} )$$

$$( \text{ j particles/sec. } )_{in} = F_j dV + ( \bar{v}_j n_j ) \, dx \, dz \qquad ( \text{III-52} )$$

$$( \text{ j particles/sec. } )_{out} = ( \bar{v}_j n_j + \bar{v}_j \frac{\partial n_j}{\partial y} \, dy ) \, dx \, dz \qquad ( \text{III-53} )$$

$$( \text{ accumulation of j particles } ) = \frac{\partial}{\partial t} ( n_j dV ). \qquad ( \text{III-54} )$$

Combining Equations ( III-51,52,53, and 54 ) according to Equation ( III-50 ) give

$$( \text{ change due to coagulation } ) dV + F_j dV + ( \bar{v}_j n_j ) \, dx \, dz$$

$$- ( \bar{v}_j n_j ) \, dx \, dz - ( \bar{v}_j \frac{\partial n_j}{\partial y} ) \, dx \, dy \, dz = \frac{\partial}{\partial t} ( n_j dV ). \qquad ( \text{III-55} )$$

Simplification of Equation ( III-55 ) and substitution of Equation ( III-47 ) gives

$$\frac{\partial n_j}{\partial t} = F_j + 2\pi \sum_{\substack{i=1 \\ m=j-i}}^{k=j-1} D_{i,m} R_{i,m} n_i n_m - 4\pi n_j \sum_{m=1}^{k} D_{j,m} R_{j,m} n_m$$

$$- \bar{v}_j \frac{\partial n_j}{\partial y}. \qquad ( \text{III-56} )$$

Equation ( III-56 ) represents the system of differential equations describing a coagulating and sedimenting polydisperse aerosol with feed.

Equation ( III-56 ) is modified using the following dimensionless variables

$$\nu_j = \frac{n_j}{N} \qquad\qquad ( \text{III-57} )$$

and

$$\tau = \frac{\bar{k} T N}{3 \bar{\mu}} t \qquad\qquad ( \text{III-58} )$$

$\nu_j$ = dimensionless particle concentration

$N$ = a reference particle number density, such as the total number of particles per unit volume

$\tau$ = dimensionless coagulation time

$T$ = absolute temperature

$\bar{k}$ = Boltzmann's constant

$\bar{\mu}$ = viscosity.

Upon treatment of Equation ( III-56 ) with Equations ( III-57 ) and ( III-58 ) and introduction of the Stokes-Cunningham correction, one

obtains ( see Appendix B )

$$\frac{\partial \nu_j}{\partial \tau} = I_j + \sum_{\substack{i=1 \\ m=j-i}}^{k=j-1} Z_{i,m} \nu_i \nu_m - 2\nu_j \sum_{m=1}^{k} Z_{j,m} \nu_m$$

$$- \left( 1 + A_j \frac{\lambda}{r_j} \right)\left( \frac{r_j}{r_1} \right)^2 \frac{\partial \nu_j}{\partial \gamma} \qquad ( III\text{-}59 )$$

where

$$I_j = F_j \frac{3\bar{\mu}}{\bar{k} T N^2} \quad = \text{dimensionless feed}$$

$$Z_{i,m} = \frac{D_{i,m} R_{i,m}}{\left( \dfrac{\bar{k} T}{6\pi\bar{\mu}} \right)} \quad = \text{dimensionless coagulation coefficient}$$

$A_j = $ coefficient in Stokes–Cunningham correction ( see Equation ( III-49 ))

$\lambda = $ mean free path of air

$$\gamma = \frac{3\bar{k} T N y}{2\pi r_1^2 \rho g} \quad = \text{dimensionless length}$$

$r_1 = $ radius of smallest particle.

Recognizing that ( see Appendix B )

$$( 1 + A_j \frac{\lambda}{r_j} )( \frac{r_j}{r_1} )^2 = j^{2/3} + 1.257 ( \frac{\lambda}{r_1} ) j^{1/3} +$$

$$.400 \, j^{1/3}( \frac{\lambda}{r_1} ) \, e^{-1.10 \, j^{1/3}( \frac{r_1}{\lambda} )}$$

$$( III-60 )$$

Equation ( III-59 ) becomes

$$\frac{\partial \nu_j}{\partial \tau} = I_j + \sum_{\substack{i=1 \\ m=j-i}}^{k=j-1} Z_{i,m} \nu_i \nu_m - 2 \nu_j \sum_{m=1}^{k} Z_{j,m} \nu_m -$$

$$\left\{ j^{2/3} + 1.257 ( \frac{\lambda}{r_1} ) j^{1/3} + .400 \, j^{1/3}( \frac{\lambda}{r_1} ) \right.$$

$$\left. e^{-1.10 \, j^{1/3} ( \frac{r_1}{\lambda} )} \right\} \frac{\partial \nu_j}{\partial \gamma} . \qquad ( III-61 )$$

For the steady state case, the transient term $(\partial \nu_j / \partial \tau)$ is set equal to zero and Equation ( III-61 ) becomes

$$\frac{d\,v_j}{d\gamma} = \left[ I_j + \sum_{\substack{i=1 \\ m=j-i}}^{k=j-1} Z_{i,m} v_i v_m - 2v_j \sum_{m=1}^{k} Z_{j,m} v_m \right] \Bigg/$$

$$\left[ j^{2/3} + 1.257 \left(\frac{\lambda}{r_1}\right) j^{1/3} + .400 \left(\frac{\lambda}{r_1}\right) j^{1/3} \right.$$

$$\left. e^{-1.10\, j^{1/3} \left(\frac{r_1}{\lambda}\right)} \right] \qquad\qquad ( \text{III-62} )$$

which is the final equation of interest.

## CHAPTER IV

## NUMERICAL PROCEDURE

### Preliminary Details and Investigations

The dimensionless coagulation equation with feed and sedimentation terms was derived as ( see Equation( III-61 ))

$$\frac{\partial \nu_j}{\partial \tau} = I_j + \sum_{\substack{i=1 \\ m=j-i}}^{k=j-1} Z_{i,m} \nu_i \nu_m - 2\nu_j \sum_{m=1}^{k} Z_{j,m} \nu_m -$$

$$\left( j^{2/3} + 1.257 \left( \frac{\lambda}{r_1} \right) j^{1/3} + .400 \left( \frac{\lambda}{r_1} \right) j^{1/3} \right.$$

$$\left. e^{-1.10\, j^{1/3} \left( \frac{r_1}{\lambda} \right)} \right) \frac{\partial \nu_j}{\partial \gamma} \qquad ( \text{IV-1} )$$

where ( see Appendix C )

$$Z_{i,m} = \frac{D_{i,m} R_{i,m}}{\left( \dfrac{\bar{k}\,T}{6\pi\bar{\mu}} \right)} = \left[ i^{1/3} + m^{1/3} \right] \times$$

$$\left[ \frac{i^{1/3} + \dfrac{\lambda}{r_1} \left( 1.257 + .400\, e^{-1.10\, i^{1/3} \frac{r_1}{\lambda}} \right)}{i^{2/3}} \right. +$$

$$\left. \frac{m^{1/3} + \frac{\lambda}{r_1}\left(1.257 + .400\,e^{-1.10\,m^{1/3}\frac{r_1}{\lambda}}\right)}{m^{2/3}} \right] =$$

the dimensionless coagulation coefficient    ( IV-2 )

and

$$I_j = F_j\ \frac{3\,\bar{\mu}}{\bar{k}\,T\,N^2} = \text{dimensionless feed}$$

$$\nu_j = \nu_i = \nu_m = \text{dimensionless concentrations}$$

$$\tau = t\ \frac{\bar{k}\,T\,N}{3\,\bar{\mu}} = \text{dimensionless time}$$

$$\lambda = \text{mean free path of air}$$

$$\gamma = \frac{3\,\bar{k}\,T\,N\,y}{2\pi r_1^2\,\rho\,g} = \text{dimensionless length.}$$

A fourth-order Runge-Kutta method was selected as the integration technique to be used because of its ease of programming and stable nature. This method, however, required large amounts of time and calculation in comparison with some predictor-corrector methods. Hidy ( 7 ) found that certain instabilities resulted at a particle size parameter of $\lambda/r_1 = 10.0$, using the predictor-corrector method of Hamming ( 12 ). Since calculations would be carried out at $\lambda/r_1 = 10.0$, time and calculations were sacrificed for stability.

As a check on the numerical proceedure, it was decided to investigate

Equation ( IV-1 ) without the feed or settling terms since a check could be made against work done by Hidy ( 7 ). This would result in solution of the equation

$$\frac{d\nu_j}{d\tau} = \sum_{\substack{i=1 \\ m=j-i}}^{k=j-1} Z_{i,m}\nu_i\nu_m - 2\nu_j\sum_{m=1}^{k} Z_{j,m}\nu_m. \qquad (\text{IV-3})$$

An upper limit of k=400 different "type" particles was selected to duplicate Hidy's work. This would necessitate a computer program to solve four-hundred simultaneous differential equations. An example of one differential equation is ( for j=5 )

$$\frac{d\nu_5}{d\tau} = \left( Z_{1,4}\nu_1\nu_4 + Z_{2,3}\nu_2\nu_3 + Z_{3,2}\nu_3\nu_2 + Z_{4,1}\nu_4\nu_1 \right) -$$

$$2\nu_5\left( Z_{5,1}\nu_1 + Z_{5,2}\nu_2 + Z_{5,3}\nu_3 + \ldots + Z_{5,400}\nu_{400} \right). \qquad (\text{IV-4})$$

The first set of terms within parenthesis represents the formation of "type 5" particles by coagulation of smaller particles. The second set of terms represents the loss of "type 5" particles by their coagulation with particles of all sizes. Calculation of the $Z_{i,m}$ , $Z_{j,m}$ coefficients can be accomplished by substitution of the correct numerical subscripts and the value of $\lambda/r_1$ into Equation ( IV-2 ).

The programming technique for the dimensionless coagulation coefficients can be found in Appendix D. These were written on tape and manipulated by the main program.

## Comparison with Previous Work

A main program was written to read and manipulate the dimension-
less gain and loss term coefficients according to Equation ( IV-3 ).
The same initial conditions were imposed on Equation ( IV-3 ) that
Hidy ( 7 ) used. These were

$$\text{at } \tau = 0, \quad \nu_1 = 1.00, \nu_{2-400} = 0.0. \qquad ( \text{ IV-5 } )$$

In addition, $\lambda/r_1 = 1.00$ was selected for comparison with the dimension-
less time increment, $\Delta\tau$, equal to 0.20 . Hidy used a dimensionless time
increment equal to 0.25 because he was integrating to a much larger
value of $\tau$ than this work was intending to go.

Execution errors occured in the initial runs because some values
of $\nu$ were smaller than machine capacity. A trapping procedure was
employed which tested the values of $\nu$ before they could cause an under-
flow problem. Referring to Equation ( IV-3 ), the product of $\nu_i \nu_m$ in the
gain summation was separated and one value of $\nu$ multiplied by a factor
of $10^{70}$. This product was then multiplied by the remaining value of $\nu$
and tested. If the final product was greater than 1.00 , the calculations
proceeded unaltered. If the final product was less than 1.00, the smal-
ler of the two values of $\nu$ was set equal to zero. The loss summation did
not produce this problem. In addition, the program calculated the total
dimensionless mass at the end of each dimensionless time increment. This
indicated whether mass was being lost from the system. The program can
be found in Appendix F.

Figure 6 shows the results obtained by Hidy ( 7 ). For comparison,
our results for Equation ( IV-3 ) and the same initial conditions with
$\Delta\tau = 0.20$ are presented in Figure 7. The agreement is very good. It
was also found that the dimensionless mass remained constant at 1.00
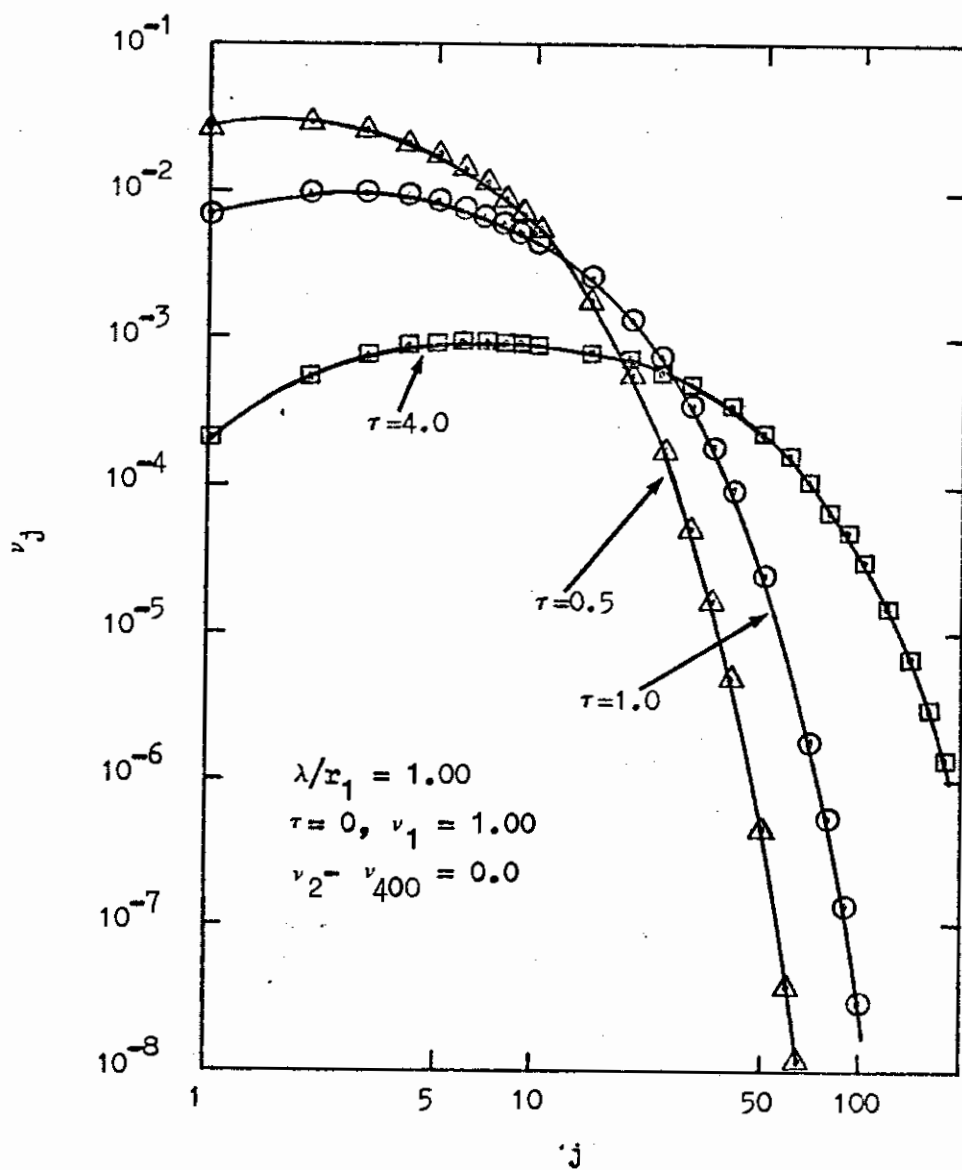
Figure 6. Hidy's Particle Size Distribution from Solution of the Coagulation
Equation ( 7 )
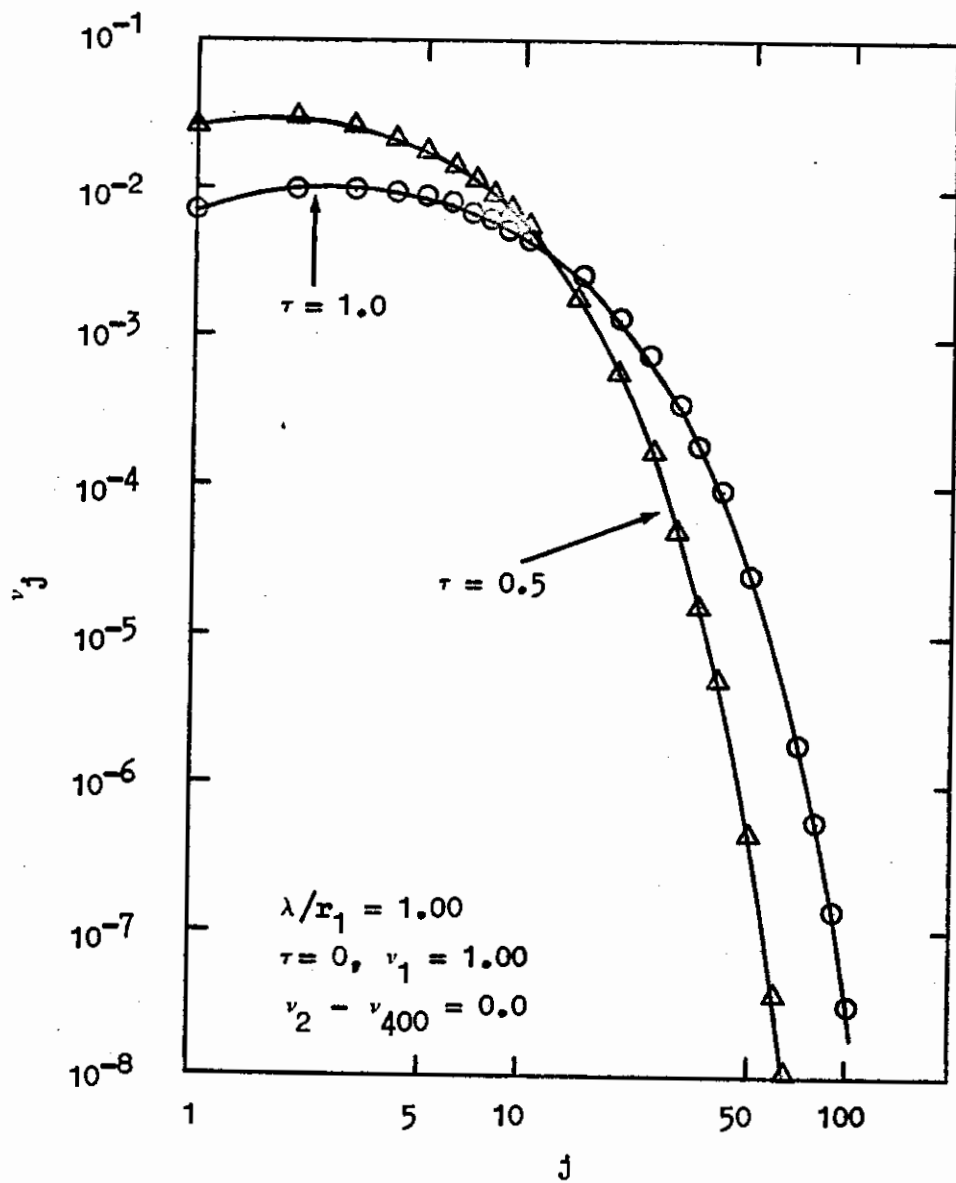
Figure 7. Particle Size Distribution from Solution of the
Coagulation Equation for Comparison with Hidy's
Solution

for each increment. Derivation of the equation used to calculate dimension-less masses can be found in Appendix H.

It was evident that the program was functioning properly. The next step was conversion of the program to solve Equation ( IV-1 ) with the transient term equal to zero.

Conversion of the Main Program to Solve the Steady State Case

With the complex tape reading and subscipt incrementing function-
ing properly, attention was turned to solving the steady state case of
Equation ( IV-1 ), rewritten below

$$\frac{d\nu_j}{d\gamma} = \left[ I_j + \sum_{\substack{i=1 \\ m=j-i}}^{k=j-1} Z_{i,m}\nu_i\nu_m - 2\nu_j\sum_{m=1}^{k} Z_{j,m}\nu_m \right] \Bigg/ $$

$$( \text{ IV-6 } )$$

$$\left[ j^{2/3} + 1.257\left(\frac{\lambda}{r_1}\right)j^{1/3} + .400\left(\frac{\lambda}{r_1}\right)j^{1/3}e^{-1.10\,j^{1/3}\left(\frac{r_1}{\lambda}\right)} \right]$$

The particle number was kept at four-hundred and the only changes
in the program were the addition of the feed term, $I_j$, and division of
the coagulation and feed terms by the dimensionless settling velocity.
The change of the independent variable from $\tau$ to $\gamma$ did not affect the
program.

## Discussion of Boundary Conditions for the Steady State Solution

In this section the various parameters and conditions that were necessary for the solution of Equation ( IV-6 ) will be discussed. These include the particle size parameter, $\lambda/r_1$, the feed term, $I_j$, the dimensionless distance increment, $\Delta\gamma$, and the dimensionless concentration, $\nu_j$.

The particle size parameter, $\lambda/r_1$, is necessary for modeling the atmospheric aerosol because it defines particle radii based on the mean free path of the diffusing medium, namely, air. The ordinate of the atmospheric size distribution ( see Figure 3 ) is spanned by three decades of particle radii, with the smallest particle radius aproximately equal to $7 \times 10^{-3}$ microns. Since the mean free path of air at $15.0^\circ$ C and 760 mm. Hg ( 18 ) is

$$\lambda = 6.63 \times 10^{-2} \text{ microns} , \qquad ( \text{IV-7} )$$

specification of $\lambda/r_1 = 10.0$ defines the smallest radius for programming use as

$$r_1 = 6.63 \times 10^{-3} \text{ microns} \qquad ( \text{IV-8} )$$

With the smallest radius defined by Equation ( IV-8 ), three decades of particle radii proceed from $6.63 \times 10^{-3}$ microns toward 6.63 microns by specifying two other segments, namely

$$\frac{\lambda}{r_1} = 1.00 , \ r_1 = 6.63 \times 10^{-2} \text{ microns}$$

$$( \text{IV-9} )$$

and

$$\frac{\lambda}{r_1} = 0.10, \quad r_1 = 6.63 \times 10^{-1} \text{ microns} \qquad ( \text{ IV--10 } )$$

for air at $15.0^{\circ}$ C and 760 mm. Hg. The size of the "type j" particle is then described as

$$r_j = \lambda(\frac{r_1}{\lambda})\sqrt[3]{j} \qquad ( \text{ IV--11 } )$$

In order to describe all discrete collisions between particles of initial radius $r_1 = 6.63 \times 10^{-3}$ microns would require $10^3$ increments of j between $\lambda/r_1 = 10.0$ and $\lambda/r_1 = 1.00$ . To descibe all discrete collisions of particles that are multiples of the unit particle ( $r_1 = 6.63 \times 10^{-3}$ microns ) and having radii between $\lambda/r_1 = 1.00$ and 0.10 would require $10^6$ increments of j. Similarly, from $\lambda/r_1 = 0.10$ to 0.01 would require $10^9$ increments of j. It is easy to see that certain compromises were necessary to keep computer time at a reasonable value.

The first compromise required that the number of different particle "types" associated with each value of $\lambda/r_1$ would be four-hundred. These would be the first four-hundred particle sizes covering the same relative position of each decade of $\lambda/r_1$ ( see Table 2 ). Secondly, in order to have four-hundred particle "types" associated with each value of $\lambda/r_1$, certain particle sizes would also be skipped when $\lambda/r_1 = 1.00$ and 0.10 . The value of $r_1$ associated with each value of $\lambda/r_1$ differed by a factor of 10 . This meant that for $\lambda/r_1 = 1.00$, each increment of j would skip 10 radii that were multiples of $6.63 \times 10^{-3}$ microns. In the same manner, the value of $r_1$ associated with $\lambda/r_1 = 0.10$ would skip 10 radii as compared to $\lambda/r_1 = 1.00$ or 100 when compared to $\lambda/r_1 = 10.0$.

These compromises were necessary in order to describe the steady state distribution as well as possible, without excessive run-time for each value of $\lambda/r_1$. Also, programs for each value of $\lambda/r_1$ would be the same except for the values of $\lambda/r_1$ which would distinguish them when read in as data.

| $\lambda/r_1 = 10.0$ $r_j = \lambda(\frac{r_1}{\lambda})\sqrt[3]{j}$ particle types increment by 1 $r_1 = 6.63 \times 10^{-3}$ microns | | $\lambda/r_1 = 1.00$ $r_j = \lambda(\frac{r_1}{\lambda})\sqrt[3]{j}$ particle types increment by 1 $r_1 = 6.63 \times 10^{-2}$ microns | | $\lambda/r_1 = 0.10$ $r_j = \lambda(\frac{r_1}{\lambda})\sqrt[3]{j}$ particle types increment by 1 $r_1 = 6.63 \times 10^{-1}$ microns | |
|---|---|---|---|---|---|
| j | $r_j$(microns) | j | $r_j$(microns) | j | $r_j$(microns) |
| 1 | $6.63 \times 10^{-3}$ | 1 | $6.63 \times 10^{-2}$ | 1 | $6.63 \times 10^{-1}$ |
| 5 | $1.14 \times 10^{-2}$ | 5 | $1.14 \times 10^{-1}$ | 5 | $1.14 \times 10^{0}$ |
| 10 | $1.43 \times 10^{-2}$ | 10 | $1.43 \times 10^{-1}$ | 10 | $1.43 \times 10^{0}$ |
| 50 | $2.44 \times 10^{-2}$ | 50 | $2.44 \times 10^{-1}$ | 50 | $2.44 \times 10^{0}$ |
| 100 | $3.09 \times 10^{-2}$ | 100 | $3.09 \times 10^{-1}$ | 100 | $3.09 \times 10^{0}$ |
| 200 | $3.89 \times 10^{-2}$ | 200 | $3.89 \times 10^{-1}$ | 200 | $3.89 \times 10^{0}$ |
| 300 | $4.46 \times 10^{-2}$ | 300 | $4.46 \times 10^{-1}$ | 300 | $4.46 \times 10^{0}$ |
| 400 | $4.90 \times 10^{-2}$ | 400 | $4.90 \times 10^{-1}$ | 400 | $4.90 \times 10^{0}$ |

Table 2. The Programming System of Particle Radii

The dimensionless distance increment, $\Delta\gamma$, was chosen to proceed in a downward direction (see Figure 5). This meant that $\gamma$ was incrementing, via integration, from an arbitrary point in the atmosphere toward the ground.

The dimensionless concentrations, $\nu_j$, also had to be specified at the zero value of $\gamma$. The selection of the boundary values for $\nu_j$ were somewhat arbitrary.

Some data on the mixing ratio of aerosols in the atmosphere are available. Figure 8 shows that at a distance of two to sixteen kilometers above the ground, the fraction of aerosols is almost four orders of magnitude smaller than at ground level. Undoubtedly, these concentration differences are significantly affected by the source, type, and size of aerosol particles that are being introduced at various altitudes. For example, at the higher altitudes natural aerosols predominate while at the lower altitudes man-made aerosols have a significant effect.

It was decided that integrations would proceed from a distance above the ground ( $\gamma = 0$ ) where the concentration of aerosols was small. Thus, $\nu_j$ for j from 1 to 400 would be set equal to zero at $\gamma$ equal to zero.

The final choice of an integration limit for the dimensionless length, $\gamma$, was determined by an allowable integration increment, available computer time, and dimensionless variables which established a relation between final values of $\gamma$ for each value of $\lambda/r_1$. Since it was necessary that the terminal values of the dimensional length, y, be the same for each value of $\lambda/r_1$, three different final values of $\gamma$ were necessary. This is demonstrated by examination of Equation ( B-10 ) rewritten below

$$\gamma = \frac{3\,\overline{k}\,T\,N}{2\pi r_1^2 \rho g}\,y \qquad\qquad ( \text{IV-12} )$$

or in terms of y

$$y = \frac{2\pi r_1^2 \rho g}{3\,\overline{k}\,T\,N}\,\gamma. \qquad\qquad ( \text{IV -13} )$$
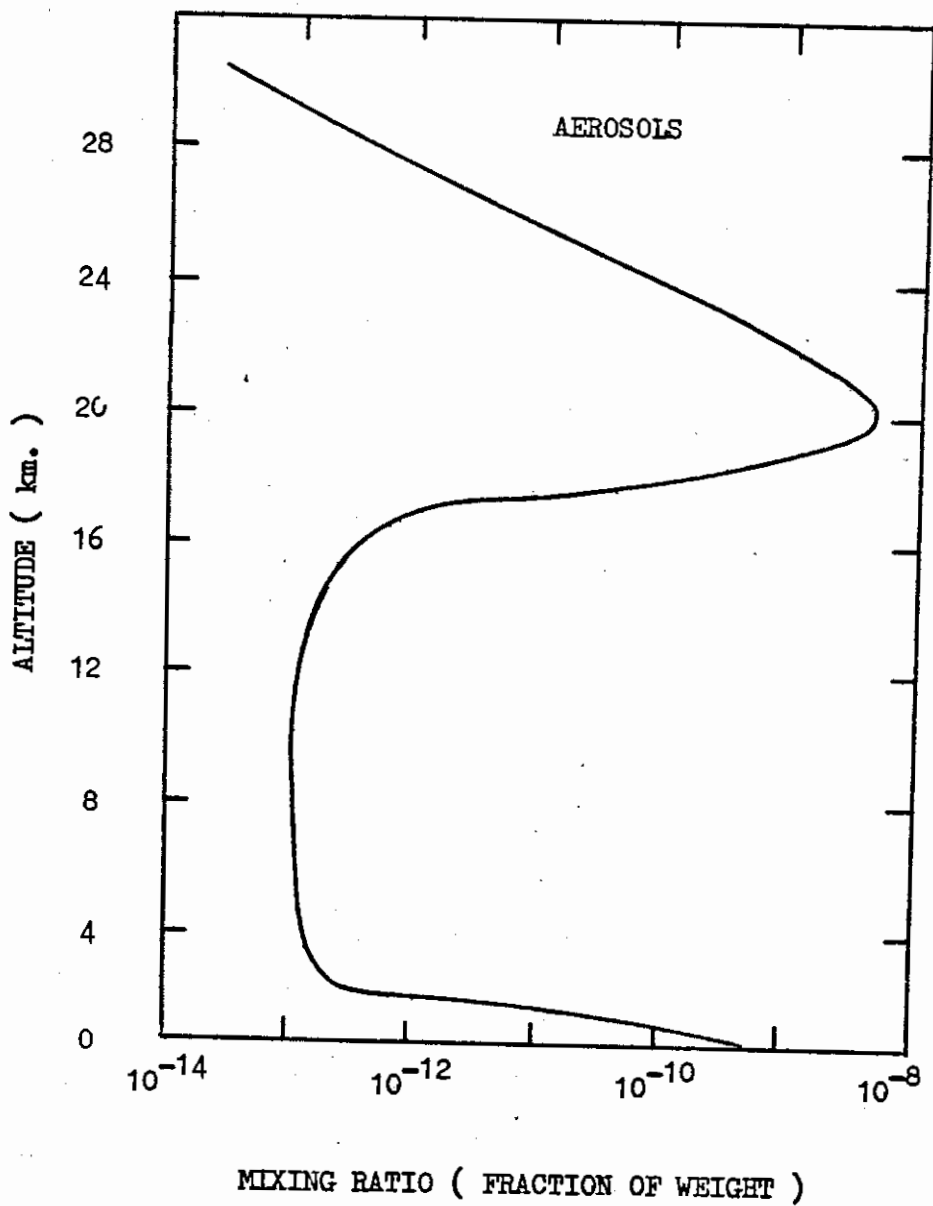
Figure 8. Mixing Ratios as a Function of Altitude ( 9 )

With a terminal value of $\gamma = 1.00$ for the segment $\lambda/r_1 = 10.0$, the value of y from Equation ( IV-13 ) is

$$y = \frac{2\pi(\frac{\lambda}{10})^2 \rho g}{3 \bar{k} T N} \ 1.00 \qquad ( \text{IV-14} )$$

It was necessary that the final value of y for the other two segments, namely, $\lambda/r_1 = 1.00$ and 0.10, be equal to that given by Equation ( IV-14 ) for $\lambda/r_1 = 10.0$ . This was required for the linkage of the three sections of $\lambda/r_1$ at the same dimensional distance. With y determined by Equation ( IV-12 ) for $\gamma = 1.00$, final values of $\gamma$ for the remaining two segments were accomplished by substitution of Equation ( IV-14 ) into Equation ( IV-12 ) with the term, $r_1^2$, in Equation ( IV-12 ) determined by the value of $\lambda/r_1$. This procedure is shown below for $\lambda/r_1 = 1.00$.

$$\gamma = \frac{3 \bar{k} T N}{2\pi(\frac{\lambda}{1.00})^2 \rho g} \ \frac{2\pi(\frac{\lambda}{10.})^2 \rho g}{3 \bar{k} T N} \ 1.00 \qquad ( \text{IV-15} )$$

$$= 0.01.$$

In a similar manner, the final value of $\gamma$ for the segment $\lambda/r_1 = 0.10$ was found to be 0.0001 .

Several trials for the integration increment, $\Delta\gamma$, showed that a value of 0.05 was stable for integrations carried out at $\lambda/r_1 = 1.00$ and 0.10. A cycling effect was seen at $\Delta\gamma$ equal to 0.05 for $\lambda/r_1 = 10.0$ which disappeared when $\Delta\gamma$ was equal to 0.025.

With terminal values of $\gamma$ determined by Equation ( IV-12 ), and acceptable values for $\Delta\gamma$ determined by trial runs, the final values of $\Delta\gamma$ and $\gamma$ for programming use were chosen to be

$$\gamma_{Final} = 1.00 \quad \text{with} \quad \Delta\gamma = 0.025 \quad \text{for} \quad \lambda/r_1 = 10.0 \qquad (\text{IV-16})$$

$$\gamma_{Final} = 0.01 \quad \text{with} \quad \Delta\gamma = 0.001 \quad \text{for} \quad \lambda/r_1 = 1.00 \qquad (\text{IV-17})$$

$$\gamma_{Final} = 0.0001 \quad \text{with} \quad \Delta\gamma = 0.00001 \quad \text{for} \quad \lambda/r_1 = 0.10 \qquad (\text{IV-18})$$

The feed term, $I_j$, was the last and most difficult value to ascertain. It was not the purpose of this research to study this facet from a physical standpoint. Since a description of the atmospheric feed has not been well defined, two completely different feed term types were chosen for investigation. These were an exponential and a constant feed type.

Since attempts would be made to link the three sections of the curve (one for each value of $\lambda/r_1$), the exponential feed type was chosen so that it would link at associated values of $\lambda/r_1$ and j. For programming purposes, the exponential type feed equation was chosen to be

$$I_j = e^{-(r_1/\lambda)\, j^{1/3}} \qquad (\text{IV-19})$$

Once again, $\lambda/r_1$ distinguished what section of the self-preserving size distribution was being described. The linking feature of the exponential feed equation is shown below.

$$\text{For} \quad \frac{\lambda}{r_1} = 10.0 \qquad \begin{aligned} I_1 &= e^{-0.10} \\ I_{1000} &= e^{-1.00} \end{aligned} \qquad (\text{IV-20})$$

$$\text{for} \quad \frac{\lambda}{r_1} = 1.00 \qquad \begin{aligned} I_1 &= e^{-1.00} \\ I_{1000} &= e^{-10.0} \end{aligned} \qquad (\text{IV-21})$$

and for $\dfrac{\lambda}{r_1} = 0.10$

$$I_1 = e^{-10.0}$$

$$I_{1000} = e^{-100.0}.$$

$(\text{IV-22})$

Of course, Equation ( IV-19 ) only describes a certain exponential distribution. No attempts were made to adjust the equation by constants, which would change the concentrations of the feed to, perhaps, conform to the atmospheric feed. The shape of the feed distribution was of more interest than the concentration of feed to each size class.

The second feed term was chosen to be a constant, i.e., all particle "types" would receive the same feed of particles. This value was set, arbitrarily, at

$$I_j = 0.10.$$

$(\text{IV-23})$

With the two widely varying feed types described by Equations ( IV-19 ) and ( IV-23 ), the coagulation equation could be studied for it's dependence upon the feed term distribution. It was hypothesized that the feed distribution would not seriously affect the shape of the steady state distribution obtained.

In conclusion, for the exponential feed type, the specified conditions were

for $\dfrac{\lambda}{r_1} = 10.0$, $1.00$, and $0.10$, $I_j = e^{-(r_1/\lambda)j^{1/3}}$

$(\text{IV-24})$

and $\gamma = 0$ for $\nu_1$ to $\nu_{400} = 0.$

For the constant feed type, the conditions were

for $\quad \dfrac{\lambda}{r_1} = 10.0, \ 1.00, \ \text{and} \ 0.10, \quad I_j = 0.10$

$$( \text{IV-25} )$$

and $\gamma = 0 \quad$ for $\quad \nu_1$ to $\nu_{400} = 0.$

A sample program printout used for the solution of Equation ( IV-6 ) is presented in Appendix G. This can be compared with that used to duplicate Hidy's work (7) in Appendix F.

Since it is not practical to describe all particle sizes in the discontinuous spectrum using today's computers, the use of three non-interacting segments represented by $\lambda/r_1 = 10.0$, $1.00$, and $0.10$ are used for this work. Because the segments are non-interacting, an attempt at exact duplication of experimental evidence found for the atmospheric self-preserving size distribution is unfeasible. The lack of experimental data for the feed term adds to the problem of numerically simulating the atmospheric self-preserving size distribution.

CHAPTER V

RESULTS AND DISCUSSION

Goals and Conditions

The goals of this chapter are to describe the results obtained for
the solution to the steady state dimensionless coagulation equation
with feed and sedimentation terms (see Equation ( III-62)). This is
rewritten below

$$\frac{d\nu_j}{d\gamma} = \left[ I_j + \sum_{\substack{i=1 \\ m=j-i}}^{k=j-1} Z_{i,m}\nu_i\nu_m - 2\nu_j\sum_{m=1}^{k} Z_{j,m}\nu_m \right] \Big/ \qquad (\text{V-1})$$

$$\left[ j^{2/3} + 1.257(\frac{\lambda}{r_1}) j^{1/3} + .400(\frac{\lambda}{r_1}) j^{1/3} e^{-1.10\, j^{1/3}(\frac{r_1}{\lambda})} \right].$$

The results are presented as plots of $\nu_j$ vs. j, as well as in a
self-preserving form. These represent the solution to Equation ( V-1 )
at a value of the dimensionless distance, $\gamma$, that corresponds to equal
values of y, the dimensional distance, for $\lambda/r_1 = 10.0$, 1.00, and 0.10
(see Equations ( IV-16, 17, and 18 )). These distributions are examined
for the effect of coagulation, sedimentation, and feed term interactions.

Distributions of $\nu_j$ vs. j represent the variation of the dimension-
less concentrations with the particle "type". For these graphs and air
at normal atmospheric conditions, "type-j" particles can be related to
their radii by the use of Table 2. However, these distributions are

based on a dimensionless volume since j is the cube of a dimensionless radius (see Equation ( III-6 )) and $v_j$ is a dimensionless concentration.

The self-preserving type plots are based on the similarity theory proposed by Swift and Friedlander ( 16 ). The results from solution of Equation ( V-1 ) are arranged into the proper form and compared to experimental evidence for the atmospheric self-preserving size distribution.

The dimensional values of $n_j$, $F_j$, and y, cannot be determined from information given in this work. Calculation of these values depends upon specification of experimental conditions such as temperature, pressure, and N, the total number of particles per unit volume.

Presentation of Results and Discussion of the Distributions for $\nu_j$ vs. j

Distributions of $\nu_j$ vs. j for the exponential feed case are pre-
sented for the segments $\lambda/r_1 = 10.0$, 1.00, and 0.10 in Figures 9, 10,
and 11, respectively. Similar plots for the constant feed case are
presented for the segments $\lambda/r_1 = 10.0$, 1.00, and 0.10 in Figures 12,
13, and 14, respectively.

In Figures 9 and 12 for $\lambda/r_1 = 10.0$, a maximum in the concentration
is observed. This is the point where the loss by sedimentation equals
the net gain by coagulation plus feed. The maximum for the exponential
feed case (Figure 9) occurs at j = 19 with $\nu_j = 8.10 \times 10^{-3}$. For particle
sizes smaller than j = 19, the net gain by coagulation plus feed is more
rapid than the losses by sedimentation while for particle sizes greater
than j = 19, the converse is true. The maximum for the constant feed
case occurs at j = 4 with $\nu_j = 2.28 \times 10^{-3}$. The maximum concentration
for the exponential feed case occurs at a larger particle size. This is
caused by the slightly larger magnitude of the exponential feed term
which results in a greater particle concentration and hence a larger
coagulation rate (see Equation ( III-43 )). The slightly greater feed to
the exponential case is also exemplified by the larger overall values of
$\nu_j$ for all values of j.

In Figures 10 and 13 with $\lambda/r_1 = 1.00$, the losses by sedimentation
are greater in magnitude than the net gain by coagulation plus feed for
both feed cases. The effect of the exponentially decreasing feed (Figure
10) is to produce a much more rapid decrease in $\nu_j$ than the constant
feed type (Figure 13).

Figures 11 and 14 for $\lambda/r_1 = 0.10$ show a very similar behavior to
their respective feed types for $\lambda/r_1 = 1.00$. The exponential feed is
producing a very rapid decrease in $\nu_j$.

In general, the effects of coagulation and sedimentation are similar
for both feed types. However, there are significant differences in the
behavior which can be directly attributed to the feed type. Specifically,
the slopes are very different, partly due to the magnitude of the feed
and also the manner by which it varies with size.
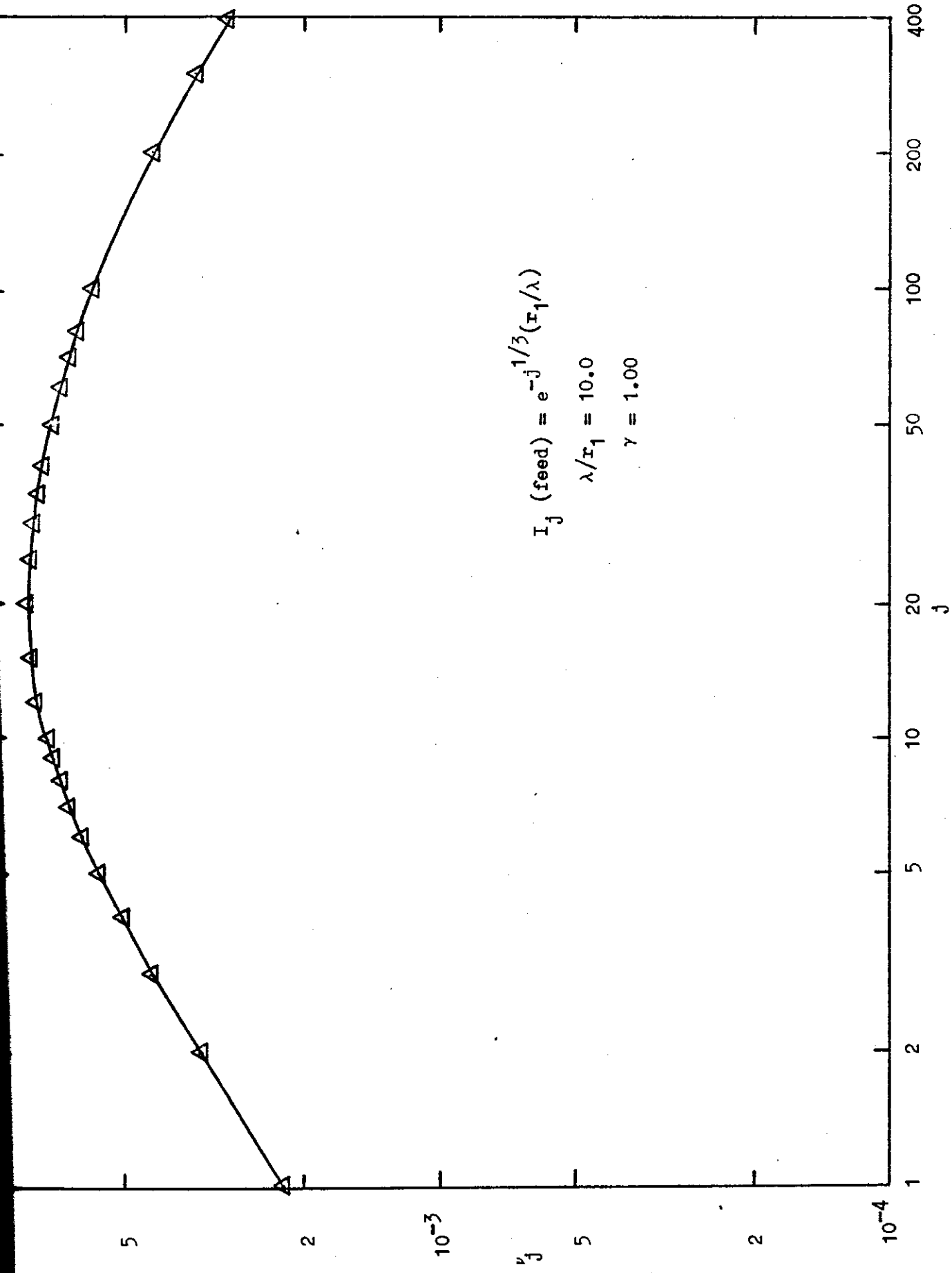
Figure 9. $\nu_j$ vs. j Distribution for $\lambda/r_1 = 10.0$, Exponential Feed

$$I_j \text{ (feed)} = e^{-j^{1/3}(r_1/\lambda)}$$

$$\lambda/r_1 = 10.0$$

$$\gamma = 1.00$$

56
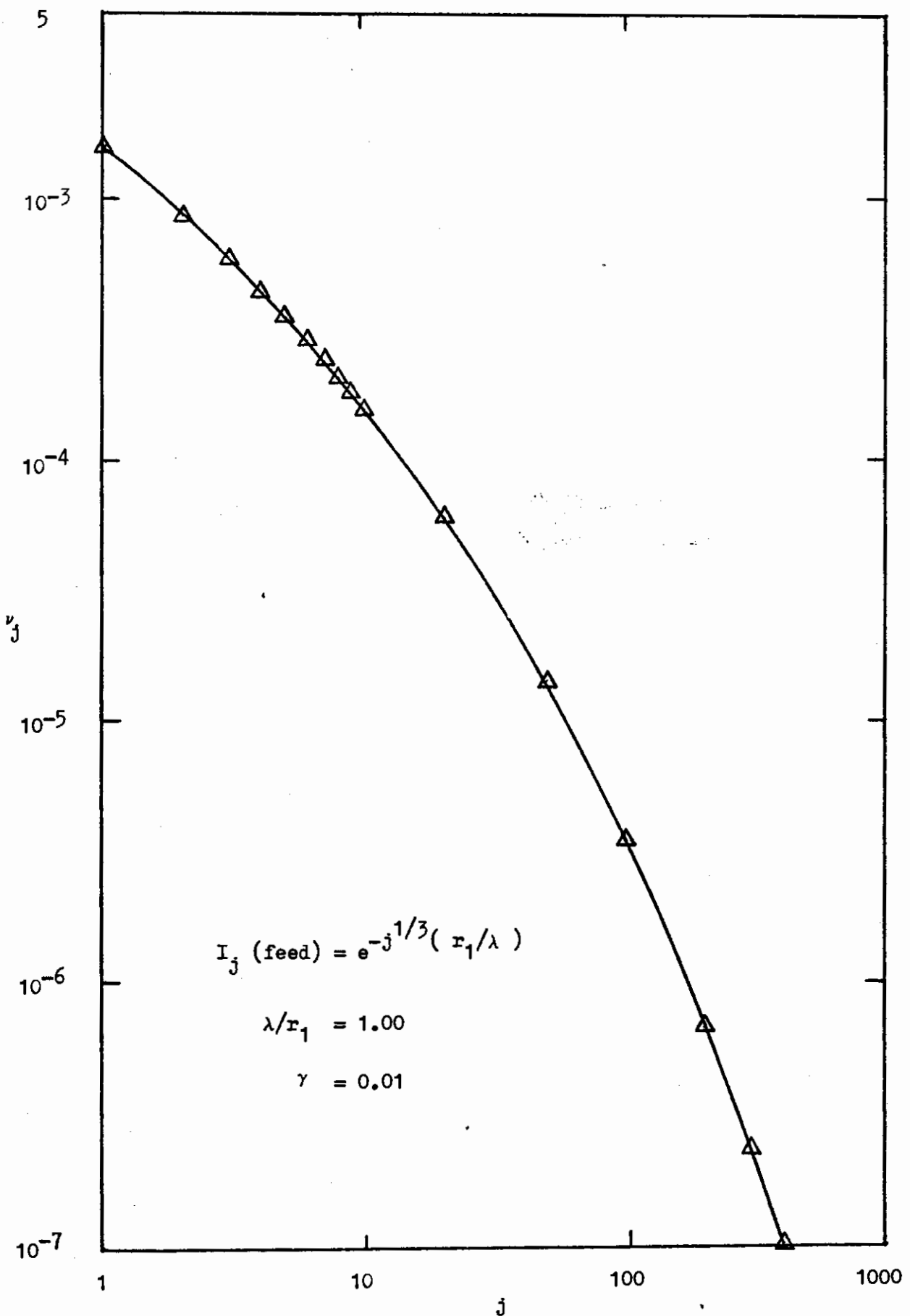
Figure 10. $\nu_j$ vs. j Distribution for $\lambda/r_1 = 1.00$, Exponential Feed
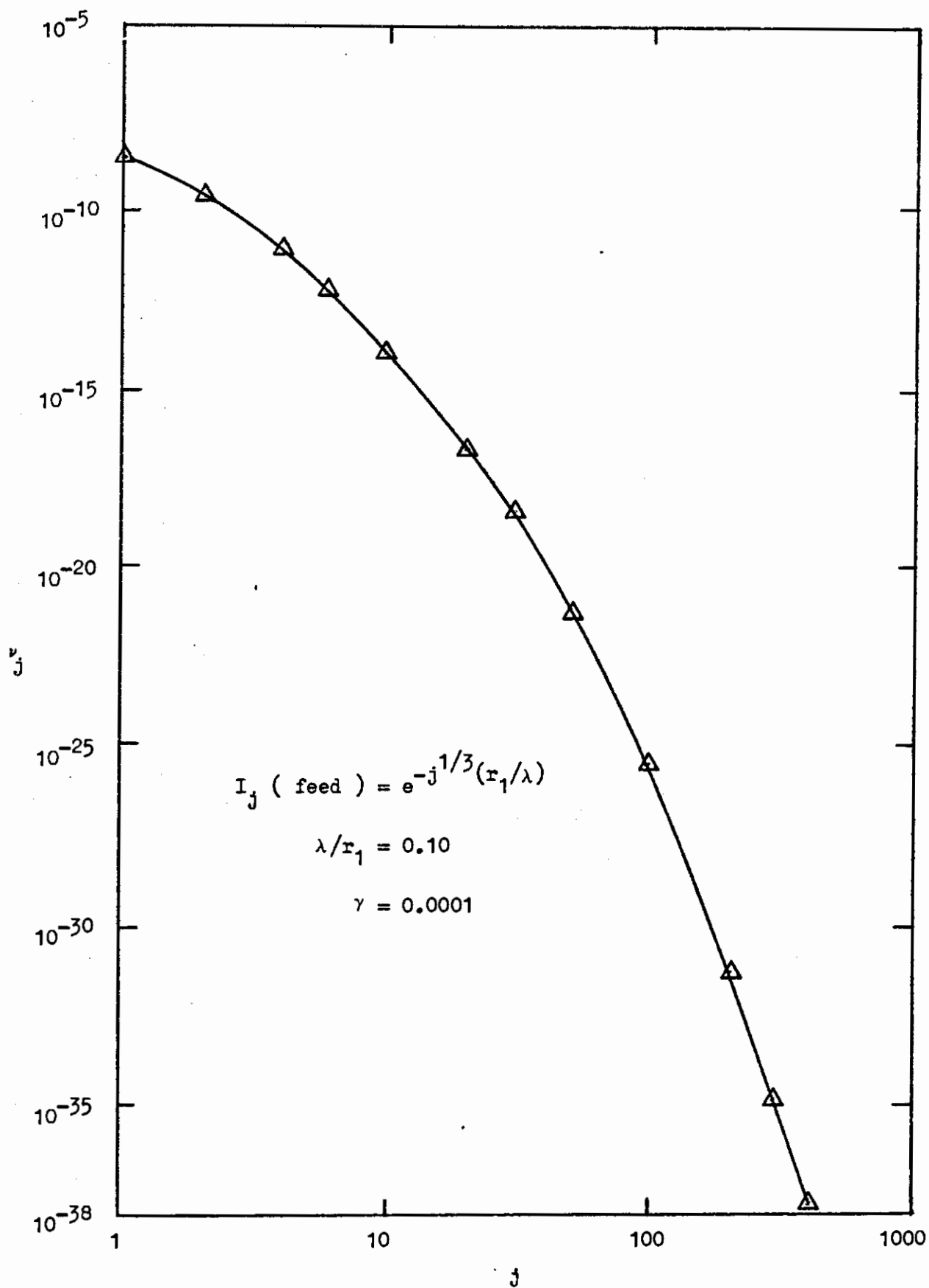
Figure 11. $\nu_j$ vs. j Distribution for $\lambda/r_1 = 0.10$, Exponential Feed

Figure 12. $\nu_j$ vs. $j$ Distribution for $\lambda/r_1 = 10.0$, Constant Feed

$I_j$ (feed) = 0.10

$\lambda/r_1 = 10.0$

$\gamma = 1.00$
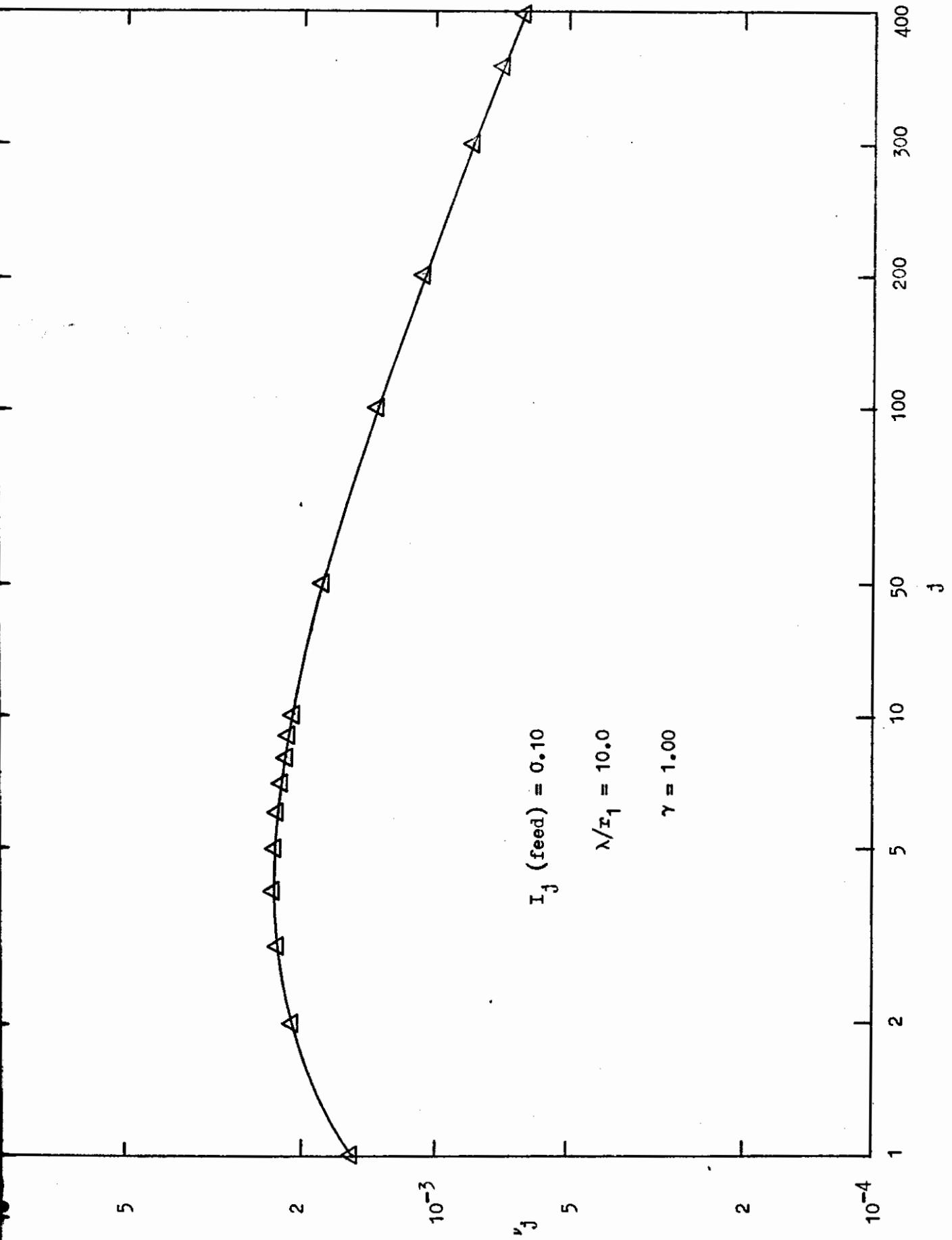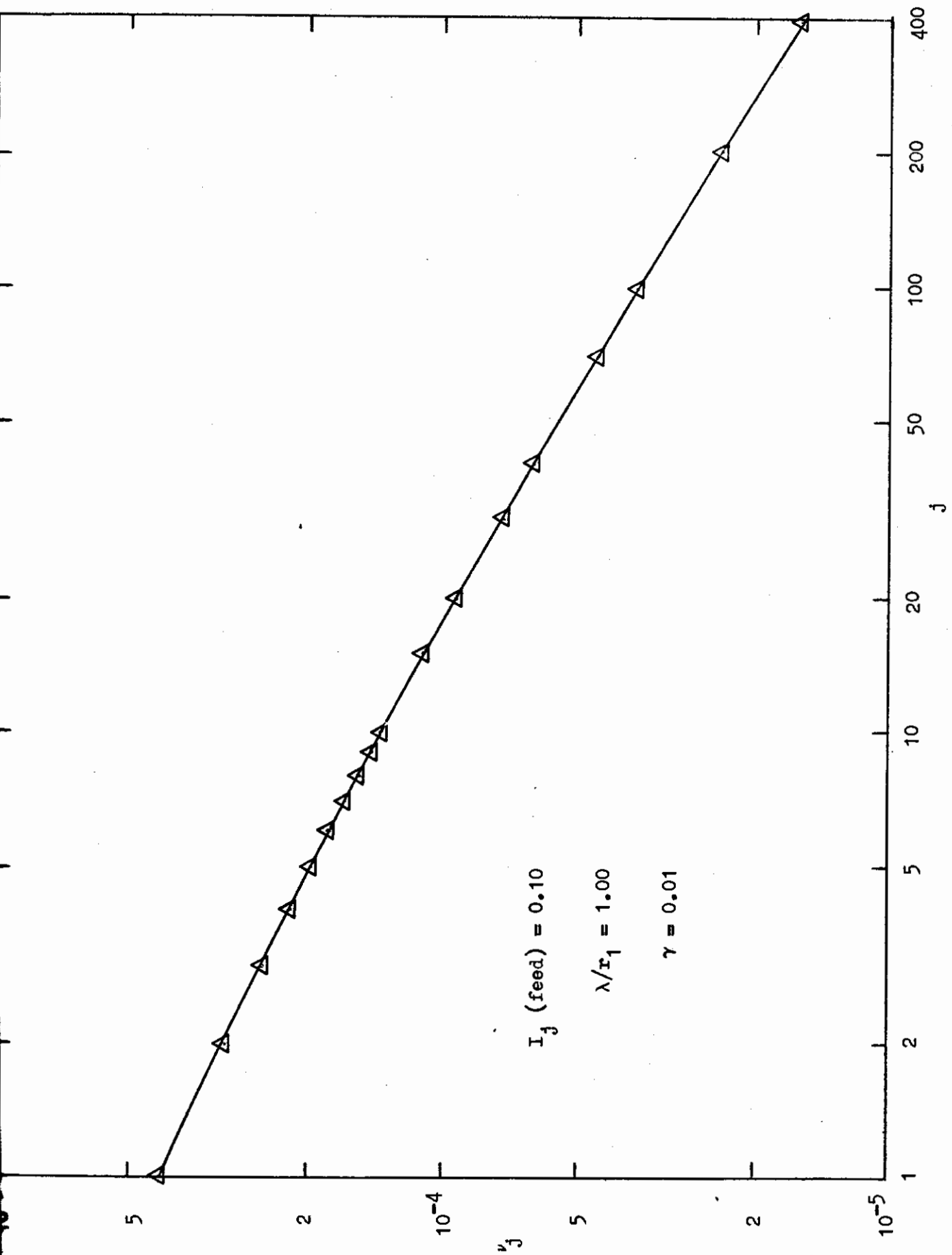
Figure 13. $\nu_j$ vs. j Distribution for $\lambda/r_1 = 1.00$, Constant Feed

$I_j$ (feed) = 0.10

$\lambda/r_1 = 1.00$

$\gamma = 0.01$

60

61
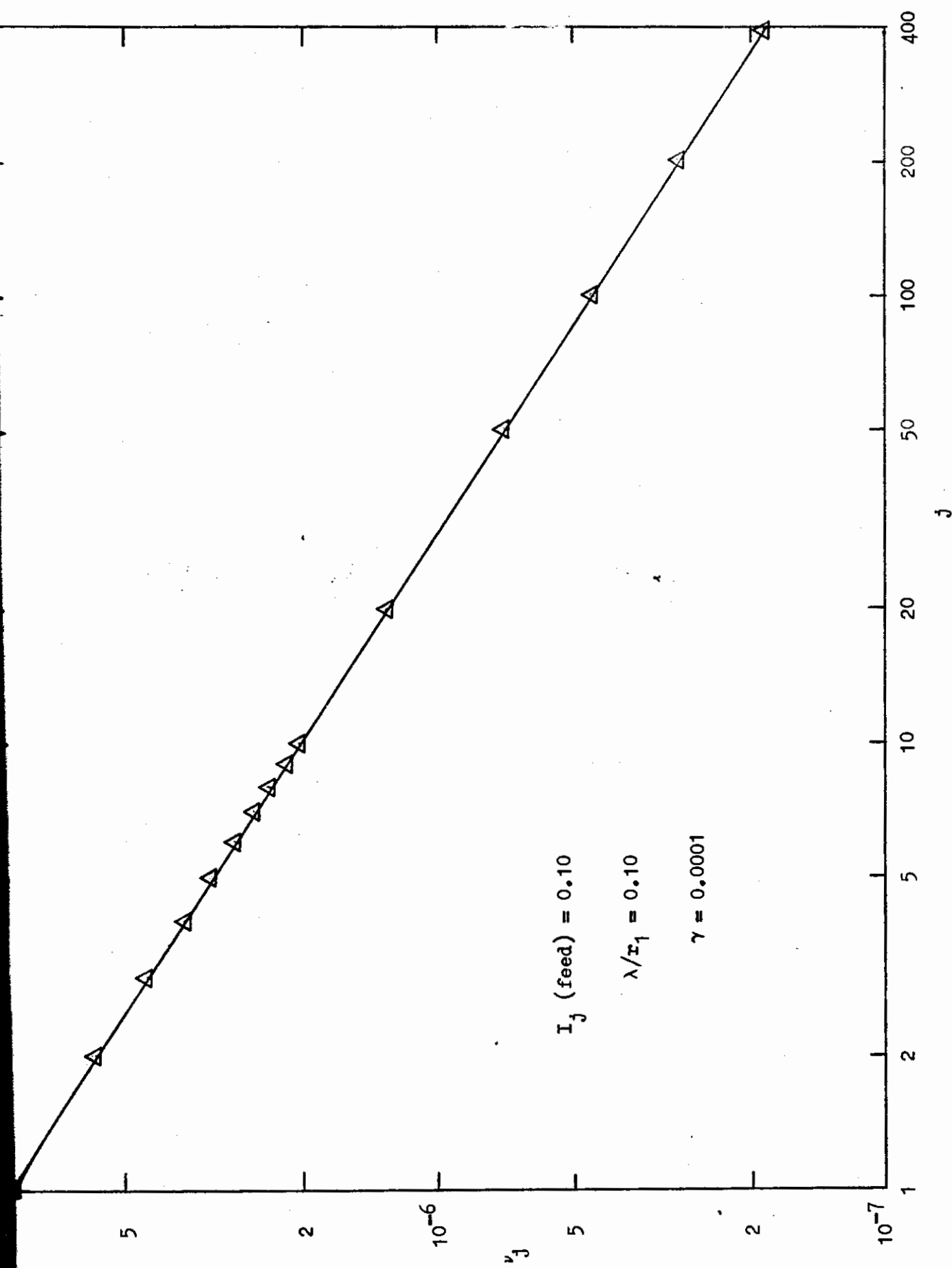


Figure 14. $\nu_j$ vs. j Distribution for $\lambda/r_1 = 0.10$, Constant Feed

$I_j$ (feed) = 0.10

$\lambda/r_1 = 0.10$

$\gamma = 0.0001$

## Presentation of Results in Self-Preserving Form

The shape of the self-preserving size distribution displayed in
Figure 3 is consistent with that shown in Figure 15. The coordinates
in Figure 15 are more suitable for this work. The dimensionless
coordinates $\psi(\eta_r)$ and $\eta_r$ are the result of the similarity theory
proposed by Swift and Friedlander ( 16 ) who tested results of oil-in-
water emulsions for self-preserving form.

The coordinates for the continuous spectrum, $\psi(\eta_r)$ and $\eta_r$, are
converted to those of the discrete spectrum and rearranged in terms of
$\nu_j$ and $j$ in Appendix J. These become

$$\psi(\eta_{r_j}) = 3\, j^{2/3}\, \nu_j \left[ \sum_s \frac{4}{3} \pi\, s\, \nu_s \right]^{1/3} \qquad ( \text{V-2} )$$

and

$$\eta_{r_j} = \frac{j^{1/3}}{\left[ \sum_s \frac{4}{3} \pi\, s\, \nu_s \right]^{1/3}}^{1/3} \qquad ( \text{V-3} )$$

where

$$\sum_s \frac{4}{3} \pi\, s\, \nu_s = \phi = \text{total volume fraction} = \text{constant.}$$

When the three segments were linked together, an alternate
method was used to calculate the dimensionless distribution
$\psi(\eta_{r_j})$ vs. $\eta_{r_j}$. This method allowed $j$ to increment in such a way
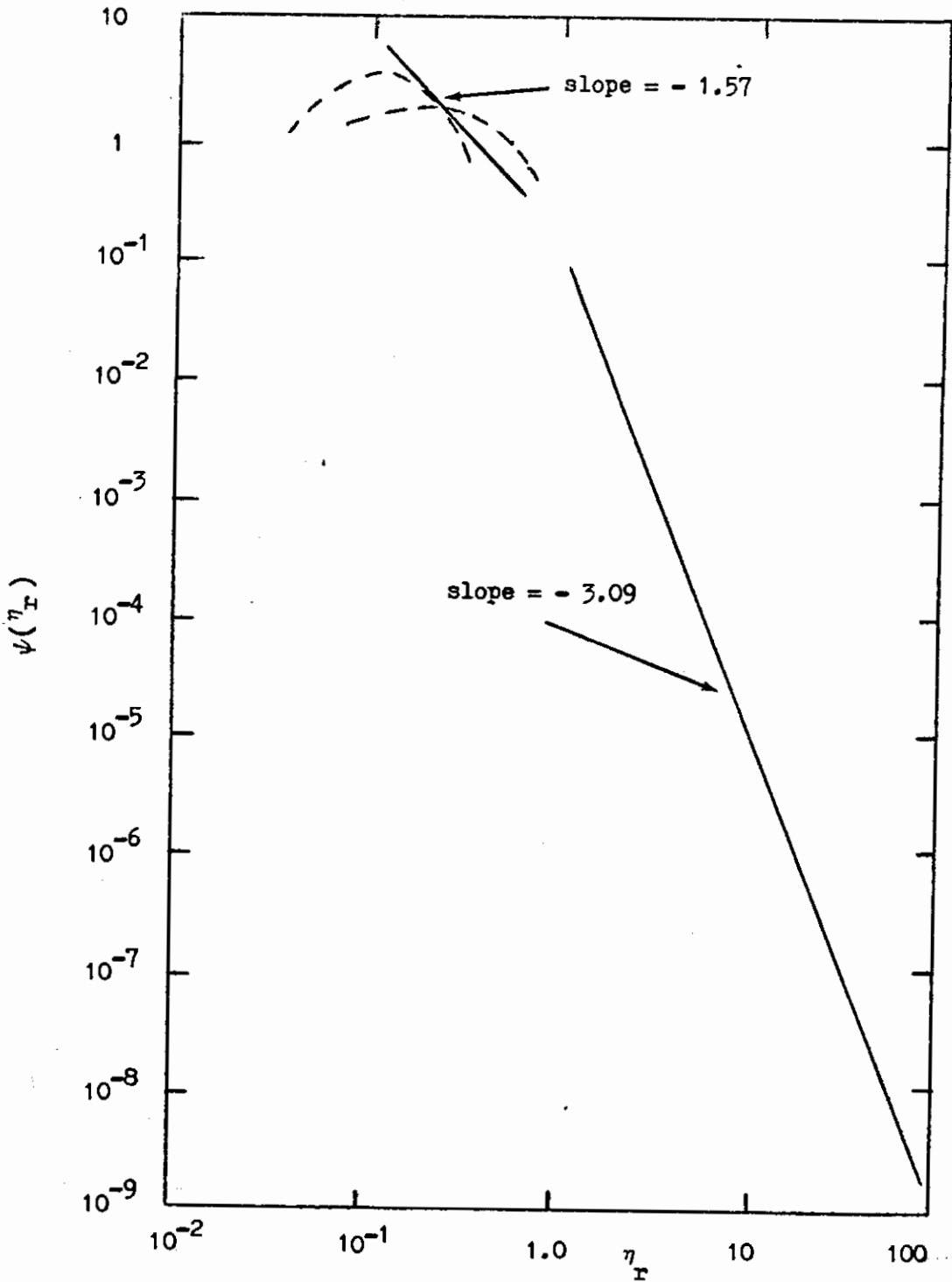
Figure 15. Self-Preserving Size Distribution for Atmospheric
Aerosols Sampled Near the Earth's Surface
(After Clark and Whitby ( 2 ))

as to replace the use of $\lambda/r_1$ in specifying larger particle sizes. This method also enabled a better visualization of the relation between $\lambda/r_1$ segments. The alternate method of incrementing j is shown in Table 3 which can be compared with Table 2 that was used for the numerical integrations. According to Table 3, for air at normal atmospheric conditions

$$r_1 \equiv 6.63 \times 10^{-3} \text{ microns} \qquad (\text{V-4})$$

and

$$r_j = r_1 \, j^{1/3}. \qquad (\text{V-5})$$

Thus, the terms $\psi(^{\eta}r_j)$ and $^{\eta}r_j$ were calculated as

$$\psi(^{\eta}r_j) = 3\,j^{2/3}\,\nu_j\left[\left(\sum_{s=1}^{400}\frac{4}{3}\pi s\,\nu_s\right)^{1/3} + \left(\sum_{s=10^3}^{400\times10^3}\frac{4}{3}\pi s\,\nu_s\right)^{1/3} + \left(\sum_{s=10^6}^{400\times10^6}\frac{4}{3}\pi s\,\nu_s\right)^{1/3}\right] \qquad (\text{V-6})$$

and

$$^{\eta}r_j = j^{1/3}\Bigg/\left[\left(\sum_{s=1}^{400}\frac{4}{3}\pi s\,\nu_s\right)^{1/3} + \left(\sum_{s=10^3}^{400\times10^3}\frac{4}{3}\pi s\,\nu_s\right)^{1/3} + \left(\sum_{s=10^6}^{400\times10^6}\frac{4}{3}\pi s\,\nu_s\right)^{1/3}\right] \qquad (\text{V-7})$$

65

| $\lambda/r_1 = 10.0$<br>$r_j = r_1\sqrt[3]{j}$<br>particle types must increment by 1<br>$r_1 = 6.63 \times 10^{-3}$ microns | | $\lambda/r_1 = 1.00$[†]<br>$r_j = r_1\sqrt[3]{j}$<br>particle types must increment by $10^3$<br>$r_1 = 6.63 \times 10^{-3}$ microns | | $\lambda/r_1 = 0.10$[†]<br>$r_j = r_1\sqrt[3]{j}$<br>particle types must increment by $10^6$<br>$r_1 = 6.63 \times 10^{-3}$ microns | |
|---|---|---|---|---|---|
| $j$ | $r_j$(microns) | $j$ | $r_j$(microns) | $j$ | $r_j$(microns) |
| 1 | $6.63 \times 10^{-3}$ | $1 \times 10^3$ | $6.63 \times 10^{-2}$ | $1 \times 10^6$ | $6.63 \times 10^{-1}$ |
| 5 | $1.14 \times 10^{-2}$ | $5 \times 10^3$ | $1.14 \times 10^{-1}$ | $5 \times 10^6$ | $1.14 \times 10^{0}$ |
| 10 | $1.43 \times 10^{-2}$ | $10 \times 10^3$ | $1.43 \times 10^{-1}$ | $10 \times 10^6$ | $1.43 \times 10^{0}$ |
| 50 | $2.44 \times 10^{-2}$ | $50 \times 10^3$ | $2.44 \times 10^{-1}$ | $50 \times 10^6$ | $2.44 \times 10^{0}$ |
| 100 | $3.09 \times 10^{-2}$ | $100 \times 10^3$ | $3.09 \times 10^{-1}$ | $100 \times 10^6$ | $3.09 \times 10^{0}$ |
| 200 | $3.89 \times 10^{-2}$ | $200 \times 10^3$ | $3.89 \times 10^{-1}$ | $200 \times 10^6$ | $3.89 \times 10^{0}$ |
| 300 | $4.46 \times 10^{-2}$ | $300 \times 10^3$ | $4.46 \times 10^{-1}$ | $300 \times 10^6$ | $4.46 \times 10^{0}$ |
| 400 | $4.90 \times 10^{-2}$ | $400 \times 10^3$ | $4.90 \times 10^{-1}$ | $400 \times 10^6$ | $4.90 \times 10^{0}$ |

[†]-for comparative purposes only, system defined by $\lambda/r_1 = 10.0$

Table 3. Alternate Method for Incrementing j

where j carried the values

$$j = 1 \text{ to } 400, \text{ incremented by } 1 \qquad\qquad ( \text{ V-8 } )$$

$$j = 10^3 \text{ to } 400 \text{ X } 10^3, \text{ incremented by } 10^3 \qquad ( \text{ V-9 } )$$

and $\quad j = 10^6 \text{ to } 400 \text{ X } 10^6, \text{ incremented by } 10^6. \qquad ( \text{ V-10 } )$

The program used to calculate the coordinates described by Equations ( V-6 ) and ( V-7 ) can be found in Appendix K.

The results of Equation ( V-1 ) for $\lambda/r_1 = 10.0$, 1.00, and 0.10, are plotted via Equations ( V-6 ) and ( V-7 ) in Figure 16 for the exponential feed case. It should be noted that the three segments have been left unjoined. Even though this work neglected interactions of particles from different $\lambda/r_1$ segments, the three segments linked together very well (no curve fitting routine necessary).

A definite similarity exists between the results of this feed case (Figure 16) and the experimental evidence for the atmospheric self-preserving size distribution (Figure 15). However, the exponential feed has definitely dropped too rapidly causing a slope which is much greater for larger particle sizes than that from experimental evidence.

The maximum value of $\psi(\eta_{rj})$ for the exponential feed case is equal to 5.8 at $\eta_{rj} = 6.0$ X $10^{-1}$. This corresponds to $j = 396$ from Table 3. The maximum value of $\psi(\eta_r)$ for the experimental plot is approximately 5.0 at $\eta_r = 10^{-1}$. This agreement is much better than anticipated.

The self-preserving plot for the constant feed case is presented in Figure 17. As with the exponential feed case, no curve fitting routine was necessary. It is very evident that when the results of the constant feed case are plotted in self-preserving form, the net coagulation rate appears greater than that of sedimentation for all particle sizes. Thus, there is a lack of a definite drop in $\psi(\eta_{rj})$ for larger particle sizes as experimental evidence indicates.

The shapes of the distributions in Figures 15, 16, and 17, are very dependent upon the total volume fraction, $\phi$, term (see Equations ( V-2 ) and ( V-3 )). In addition to affecting the coordinates of the
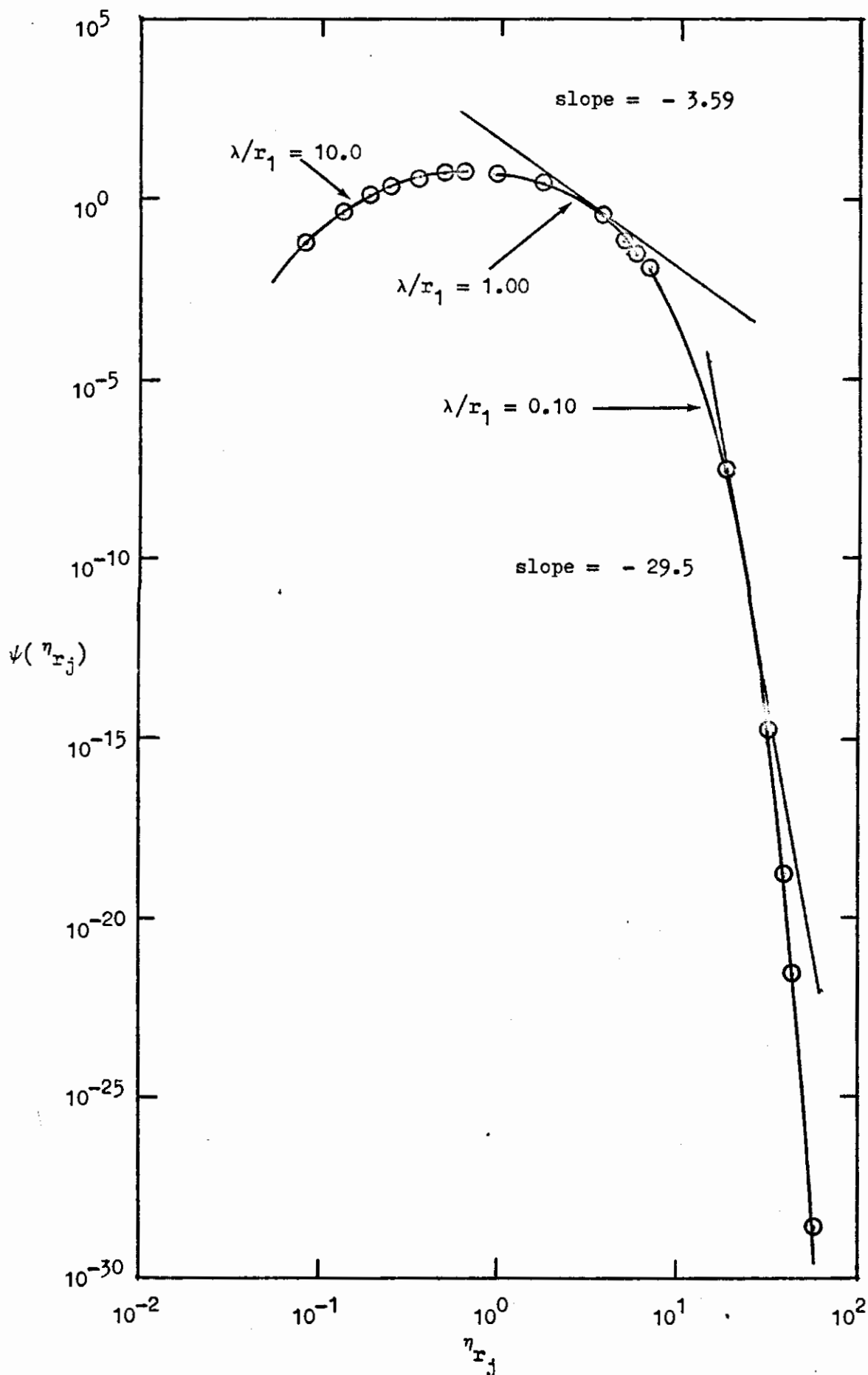
Figure 16. Self-Preserving Size Distribution from Solution of the Dimensionless Coagulation Equation with Feed and Sedimentation Terms, Exponential Feed
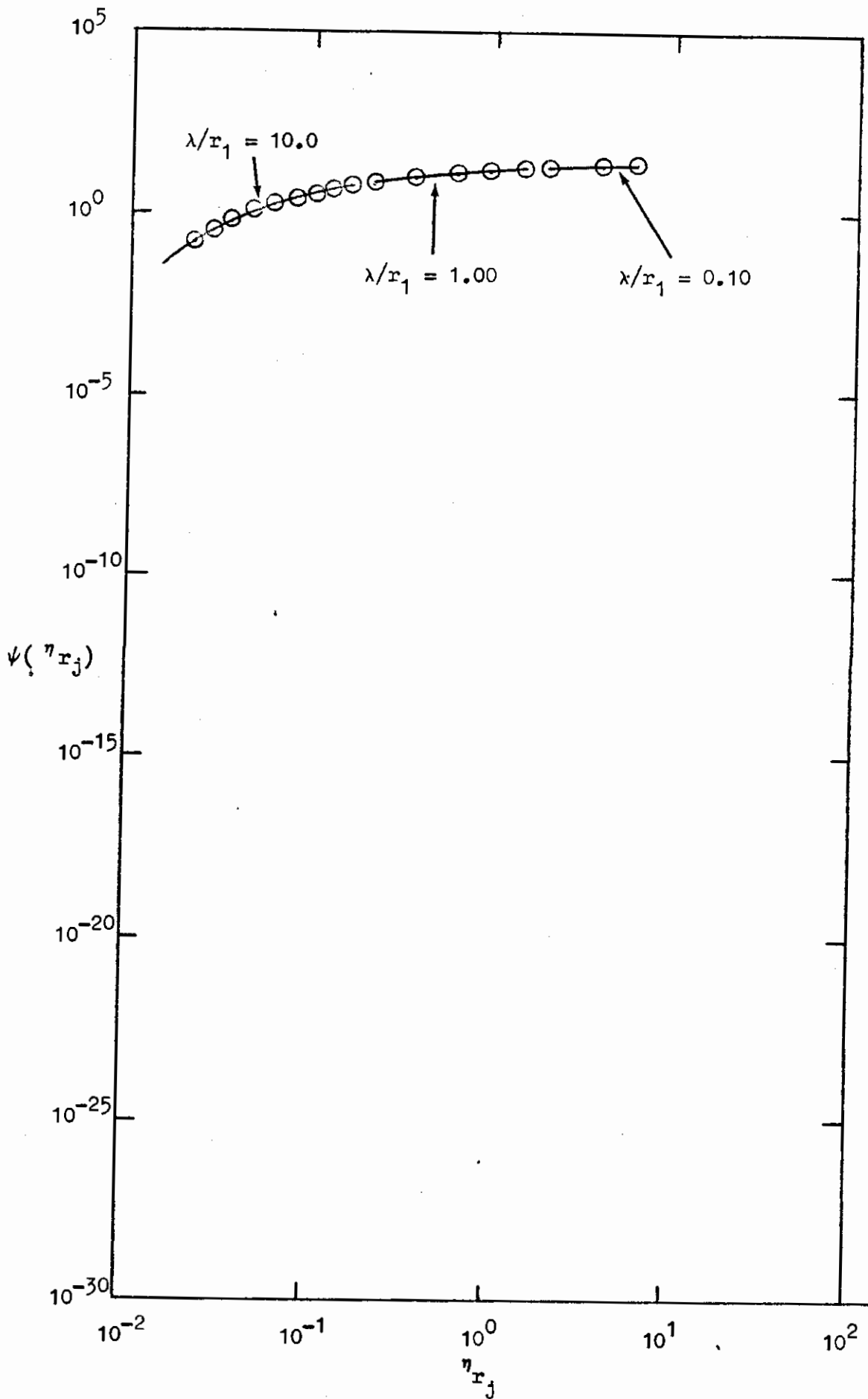
Figure 17. Self-Preserving Size Distribution from Solution of the Dimensionless Coagulation Equation with Feed and Sedimentation Terms, Constant Feed

self-preserving plot, $\phi$ also affects the coagulation rate. An increase in coagulation rate for a particular value of $\lambda/r_1$ is caused by a larger concentration of particles and hence, an increase in the magnitude of $\phi$. Thus, a description of the self-preserving plots in terms of $\phi$ is necessary.

The first plotted point for the exponential feed case (see Table 3, $j = 1$) in Figure 16 is $\psi(\eta_{r_j}) = 8.22 \times 10^{-2}$ at $\eta_{r_j} = 8.21 \times 10^{-2}$. Similarly, the first plotted point for the constant feed case is $\psi(\eta_{r_j}) = 2.12 \times 10^{-1}$ at $\eta_{r_j} = 2.17 \times 10^{-2}$ (Figure 17). Since $j = 1$ for both points, the only way in which there can be a smaller value of $\eta_{r_j}$ for the constant feed case is for $\phi$ to be larger for this feed case. The larger magnitude of $\phi$ explains the lack of a decline in $\psi(\eta_{r_j})$ values for larger particle sizes for the constant feed case; since the net rate of coagulation plus feed is greater than that of sedimentation as indicated by the larger magnitude of $\eta_{r_j}$.

Perhaps a decrease of $\psi(\eta_{r_j})$ would have been observed for the constant feed case if $I_j$ were smaller than 0.10. This would have the effect of decreasing $v_j$, and hence $\phi$, thereby increasing $\eta_{r_j}$ to values where a decrease in $\psi(\eta_{r_j})$ would be expected.

The shapes of the curves in Figures 16 and 17 are the result of an attempt at simulating the experimental evidence found for the atmospheric self-preserving size distribution. This attempt demanded many compromises and assumptions. The neglection of certain particle sizes and the use of non-interacting segments limits conclusions of the results of this work to basic shape comparisons.

CHAPTER VI

CONCLUSIONS

The following conclusions result from this study:

(1)     The form of Equation ( III-62 ) seems applicable for studying
the atmospheric self-preserving size distribution, i.e.,

$$\frac{d\nu_j}{d\gamma} = \left[ I_j + \sum_{\substack{i=1 \\ m=j-i}}^{k=j-1} Z_{i,m}\nu_i\nu_m - 2\nu_j \sum_{m=1}^{k} Z_{j,m}\nu_m \right] \Bigg/$$

$$\left[ j^{2/3} + 1.257\left(\frac{\lambda}{r_1}\right)j^{1/3} + .400\left(\frac{\lambda}{r_1}\right)j^{1/3} \right.$$

$$\left. e^{-1.10\, j^{1/3}\left(\frac{r_1}{\lambda}\right)} \right]. \qquad ( VI-1 )$$

(2)     The magnitude of the feed term, as well as its form,
affects the slopes of the self-preserving plots. An
increase in the feed term causing an increase in
coagulation rate is consistent with theory.

(3)     Because of the very good link-up of the segments for the

self-preserving plots, the interaction of particles between
segments appears to be minimal. However, the interpretation
of the apparent unimportance of the interactions are still
tentative.

(4)     The feed types chosen for this work exaggerated the effect of
the feed term as desired. However, a gradually decreasing
exponential feed or a constant feed of smaller magnitude
would appear to be more realistic feed functions for further
investigation.

CHAPTER VII

SUGGESTIONS FOR FURTHER INVESTIGATION

(1)    Since segmenting of the steady state size distribution into
       three segments did not seem to cause excessive interactions,
       further investigation of the effect of non-interacting
       segments should be continued.

(2)    A slowly decreasing exponential feed and a constant feed of
       smaller magnitude should be studied for their effect upon
       the dimensionless steady state distribution.

A SELECTED BIBLIOGRAPHY

1.  Chandrasekhar, S., "Stochastic Problems in Physics and Astronomy," Rev. Mod. Phys., 15,60-63, (1943).

2.  Clark, W., and Whitby, K.,   J. Atmos. Sci., 24 , 684, (1967).

3.  Davies, C. N., Proc. Phys. Soc. ( London ), 57, 259, (1945).

4.  Friedlander, S. K., and Wang, C. S., "The Self-Preserving Particle Size Distribution for Coagulation by Brownian Motion," J. Colloid and Interface Sci. 22, 126-132, (1966)

5.  Fuchs, N. A.,"The Mechanics of Aerosols," Pergamon Press Book Company, New York, (1964)

6.  Hidy, G. M., and Brock, J. R., "The Dynamics of Aerocolloidal Systems,"  Pergamon Press, Great Britain, (1970)

7.  Hidy, G. M., "On the Theory of the Coagulation of Noninteracting Particles in Brownian Motion," J. Colloid Sci. 20 , 123-144, (1965)

8.  Kolmogoroff, A., and Leontowitsch, M., Phys. Z. Sowjetunion 4, 1, (1933)

9.  McCormac, B. M., "Introduction to the Scientific Study of Atmospheric Pollution," D. Reidel Publishing Company, Dordrecht-Holland, (1971)

10.  Mockros, L. F., et. al., "Coagulation of a Continuously Reinforced Aerosol," <u>J. Colloid and Interface Sci.</u> <u>23</u> , 90-98, (1967)

11.  Müller, H., "Die Theorie der Koagulation Polydisperser Systeme," <u>Kolloid Zeitschrift</u> <u>38</u> , 1-2 , (1926)

12.  Ralston, A., and Wilf, H., "Mathematical Methods for Digital Computers," Wiley, New York, (1960)

13.  Smoluchowski, M. v., "Drei Vorträge über Diffusion, Brownsche Molekularbewegung und Koagulation von Kolloidteilchen," <u>Physikalische Zeitschrift</u> <u>17</u> , 558-599, (1916)

14.  Smoluchowski, M. v., "Versuch einer Mathematischen Theorie der Koagulationskinetik Kolloider Lösungen," <u>Zeitschrift Fuer Physikalische Chemie</u> <u>92</u> , 129-168 (1918)

15.  Stern, A. C., "Air Pollution," Academic Press, New York, Vol. 1, (1968)

16.  Swift, D. L., and Friedlander, S. K., "The Coagulation of Hydrosols by Brownian Motion and Laminar Shear Flow," <u>J. Colloid Sci.</u> <u>19</u> , 621-647, (1964)

17.  Wang, C. S., and Friedlander, S. K., "The Self-Preserving Particle Size Distribution for Coagulation by Brownian Motion," <u>J. Colloid and Interface Sci.</u> <u>24</u> , 170-179, (1967)

18. West, R. C., "Handbook of Chemistry and Physics," 48th. Edition, Chemical Rubber Company, (1967)

19. Zessack, U., "The Coagulation of Mixed Dusts," _Staub Reinatling Luft_ 28 , 53-60, (1968)

## NOMENCLATURE

$A_j$      coefficient in Stokes-Cunningham correction for particle "type j"

$D_{i,j}$      diffusivity of particles of "type i" and "type j"

$F_j$      feed of particles to "type j" size class

$G$      term in Stokes-Cunningham correction

$g$      acceleration of gravity

$I_j$      dimensionless feed of particles to "type j" size class

$J_{i,j}$      collision frequency between "type i" and "type j" particles

$j^*$      particle flux

$K_{i,j}$      coagulation constant for "type i" with "type j" particles

$\bar{k}$      Boltzmann's constant

$N$      total number of particles per unit volume

$n_i$      "type i" particle concentration

$R_{i,j}$      coagulation radius for particles of "type i" with "type j"

$r$      particle radius

$s^*$      surface area of coagulation radius

$T$      absolute temperature

$t$      time

$V$      volume

$\bar{v}_j$      Stokes terminal settling velocity for particle "type j"

$x$      length

$y$      length

$Z_{i,j}$     dimensionless coagulation coefficient for particles "type i" with "type j"

$z$     length

## Greek Letters

$\gamma$     dimensionless length

$\delta$     variable in Equation ( III-28 )

$\eta$     dimensionless coordinate of self-preserving size distribution plot

$\lambda$     mean free path of air

$\bar{\mu}$     viscosity

$\mu$     microns

$\nu_j$     dimensionless "type-j" particle concentration

$\xi$     variable in Equation ( III-28 )

$\rho$     density

$\sigma_{i,j}$     number of j particle contacts per i particle per unit time

$\tau$     dimensionless coagulation time

$\phi$     total volume fraction

$\psi$     dimensionless coordinate of self-preserving size distribution plot

## Subscripts

$i = j = m = s =$ intigers referring to particle "types"

$i0 = j0 =$ initial "types"

$1 =$ particle "type 1"

APPENDIX A


EFFECT OF THE NON-SUMMED TERMS ON THE SOLUTION TO THE COAGULATION EQUATION


The two extra terms, namely, Equations ( III-23 ) and ( III-24 ) were added to the program for the steady state case (see Appendix G) and tested for the conditions $\lambda/r_1 = 0.10$ and constant feed. The solution is presented in Figure 18. This can be compared to Figure 14 which is the solution of the steady state coagulation equation for the same conditions except deletion of the extra terms. A comparison of Figures 14 and 18 indicates that the non-summed terms are insignificant and can be ignored for this work.

The alteration of the main program for the purpose of testing the effect of the non-summed terms can be seen in Figure 19. This can be compared to the program found in Appendix G.
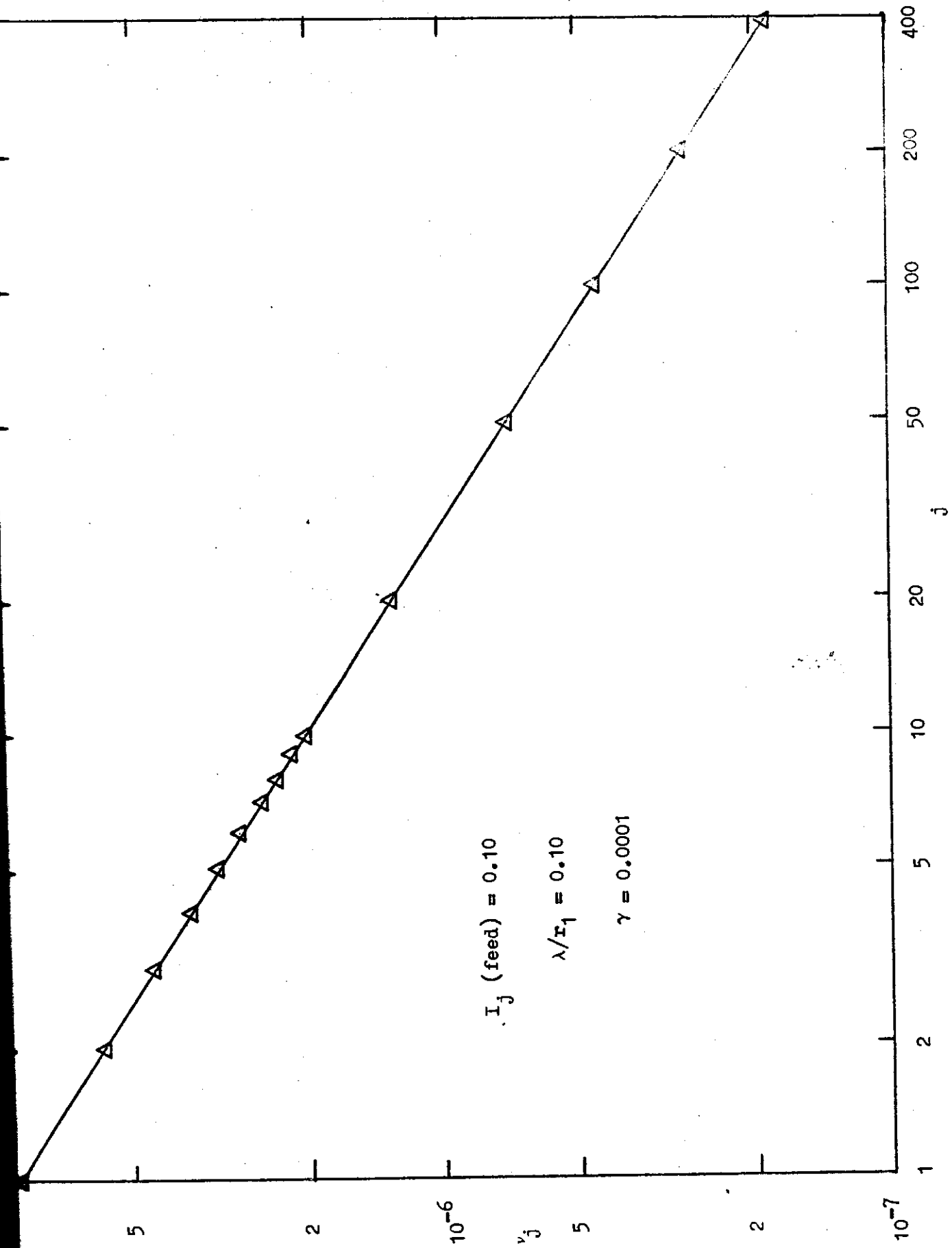
Figure 18. $\nu_j$ vs. $j$ Distribution for $\lambda/r_1 = 0.10$, Constant Feed-EXTRA TERMS

$I_j$ (feed) = 0.10

$\lambda/r_1 = 0.10$

$\gamma = 0.0001$

79

```
       DIMENSION X(400),XX(400),A(400),Q(400),D(400),F(400),T(400),K(4,40
         •
         •
         •

         •
  18   IX=((II-1)*KMAX-(II-1)**2)+JJ-II+1
       A(M)=A(M)+C(IX)*X(II)*X(JJ)
       IF(II .LT. JJ)GO TO 13
       IVV=II/2
       IX=((IVV-1)*KMAX-(IVV-1)**2)+1
       A(M)=A(M)+(C(IX)*X(IVV)*X(IVV))/2
  13   GO TO 7
         •
         •
         •

         •
  14   DO 94 JJ=1,KMAX
       NN=KK
       KK=KK-20*M
       Q(NN)=Q(NN)+Z(JJ,KK)*X(JJ)
       IF(NN .EQ. JJ)Q(NN)=Q(NN)+Z(JJ,KK)*X(JJ)
       KK=KK+20*M
  94   CONTINUE
         •
         •
         •

         •

         •
       END
```

Figure 19. Alteration of the Main Program for the Purpose of Testing
the Effect of the Non-Summed Polydisperse Coagulation Terms

APPENDIX B

NON-DIMENSIONALIZATION OF THE COAGULATION EQUATION

The coagulation equation for a sedimenting aerosol( Equation III-56 ) is

$$\overset{①}{\partial n_j/\partial t} = \overset{②}{F_j} + 2\pi\overset{k=j-1}{\underset{\substack{i=1 \\ m=j-i}}{\sum}}\overset{③}{D_{i,m}R_{i,m}n_i n_m} \; - 4\pi n_j \overset{k}{\underset{m=1}{\sum}}\overset{④}{D_{j,m}R_{j,m}n_m}$$

$$- \bar{v}_j \overset{⑤}{\partial n_j/\partial y} \; . \qquad\qquad ( B-1 )$$

Let
$$\nu_j = n_j/N \qquad\qquad ( B-2 )$$
and
$$\tau = \bar{k}TNt/3\bar{\mu}. \qquad\qquad ( B-3 )$$

The treatment of Equation( B-1 ) with Equations ( B-2 ) and ( B-3 ) produces

① $\qquad \partial n_j/\partial t = \dfrac{\bar{k}TN^2}{3\bar{\mu}}\dfrac{\partial \nu_j}{\partial \tau}$ $\qquad\qquad ( B-4 )$

② $\qquad F_j \dfrac{3\bar{\mu}}{\bar{k}TN^2} \; \equiv \; I_j$ $\qquad\qquad ( B-5 )$

③ $\qquad 2\pi\overset{k=j-1}{\underset{\substack{i=1 \\ m=j-i}}{\sum}}D_{i,m}R_{i,m}n_i n_m \quad \dfrac{3\bar{\mu}}{NN\bar{k}T} \quad =$

$$\frac{6\pi\bar{\mu}}{\overline{k}T}\sum_{\substack{i=1 \\ m=j-i}}^{k=j-1}D_{i,m}R_{i,m}\nu_i\nu_m \qquad\qquad (\text{ B-6 })$$

④ $\quad\dfrac{-4\pi n_j}{N}\displaystyle\sum_{m=1}^{k}D_{j,m}R_{j,m}\;\dfrac{n_m}{N}\;\dfrac{3\bar{\mu}}{\overline{k}T}\qquad\qquad=$

$$\frac{-12\pi\bar{\mu}\nu_j}{\overline{k}T}\sum_{m=1}^{k}D_{j,m}R_{j,m}\nu_m \qquad\qquad (\text{ B-7 })$$

⑤ $\quad-\bar{v}_j\dfrac{\partial n_j}{\partial y}\;\dfrac{3\bar{\mu}}{\overline{k}TN^2}\qquad=\quad-\bar{v}_j\;\dfrac{3\bar{\mu}}{\overline{k}TN}\;\dfrac{\partial(n_j/N)}{\partial y}\qquad=$

$$-\bar{v}_j\;\frac{3\bar{\mu}}{\overline{k}TN}\;\frac{\partial\nu_j}{\partial y}. \qquad\qquad (\text{ B-8 })$$

By Stokes Law with the Cunningham correction factor( see Equation III-48 ),
for term ⑤

$$\bar{v}_j=\frac{2\pi r_j^{2}\rho g}{9\bar{\mu}}\left(1+A_j\;\frac{\lambda}{r_j}\right) \qquad\qquad (\text{ B-9 })$$

Equation ( B-9 ) is the Stokes terminal settling velocity corrected by
the Stokes-Cunningham factor. Using Equation ( B-9 ), Equation ( B-8 )
becomes

$$- \quad \frac{2\pi r_j^2 \rho g}{3\bar{k}TN} \left( 1 + A_j \ \frac{\lambda}{r_j} \right) \ \frac{\partial v_j}{\partial y} . \qquad \textbf{( B-10 )}$$

Letting
$$\gamma = \frac{3\bar{k}TNy}{2\pi r_1^2 \rho g} \qquad ( \text{ B-11 } )$$

Equation ( B-10 ) becomes

$$- \left( 1 + A_j \ \frac{\lambda}{r_j} \right) \frac{r_j^2}{r_1^2} \ \frac{\partial v_j}{\partial \left[ \dfrac{3\bar{k}TNy}{2r_1^2 \rho g} \right]} \qquad ( \text{ B-12 } )$$

or

$$- \left( 1 + A_j \ \frac{\lambda}{r_j} \right) \left( \frac{r_j}{r_1} \right)^2 \ \frac{\partial v_j}{\partial \gamma} . \qquad ( \text{ B-13 } )$$

Equation ( B-1) now becomes

$$\frac{\partial v_j}{\partial \tau} \ = \ I_j \ + \ \frac{6\pi\bar{\mu}}{\bar{k}T} \sum_{\substack{i=1 \\ m=j-i}}^{k=j-1} D_{i,m} R_{i,m} v_i v_m \ - \ \frac{12\pi\bar{\mu}}{\bar{k}T} \ v_j$$

$$\sum_{m=1}^{k} D_{j,m} R_{j,m} v_m \ - \ \left( 1 + A_j \ \frac{\lambda}{r_j} \right) \left( \frac{r_j}{r_1} \right)^2 \frac{\partial v_j}{\partial \gamma} \ ( \text{ B-14 } )$$

84

Now ( see Equations ( III-45 ) and ( III-46 )

$$D_{i,m} = D_i + D_m \qquad (B\text{-}15)$$

and

$$R_{i,m} = r_i + r_m \qquad (B\text{-}16)$$

while for Brownian motion, the diffusivity is given by the Stokes-Einstein relation ( 5 )

$$D_i = \frac{\bar{k}T}{6\pi\bar{\mu}r_i}\left(1 + A_j \frac{\lambda}{r_j}\right). \qquad (B\text{-}17)$$

Thus

$$D_{i,m}R_{i,m} = \frac{\bar{k}T}{6\pi\bar{\mu}}\left(\frac{1}{r_i} + A_i \frac{\lambda}{r_i^2} + \frac{1}{r_m} + A_m \frac{\lambda}{r_m^2}\right)$$
$$(r_i + r_m) \qquad (B\text{-}18)$$

and $Z_{i,m}$ is defined as

$$Z_{i,m} \cong \frac{D_{i,m}R_{i,m}}{\left[\frac{\bar{k}T}{6\pi\bar{\mu}}\right]} = \left(\frac{1}{r_i} + A_i \frac{\lambda}{r_i^2} + \frac{1}{r_m} + A_m \frac{\lambda}{r_m^2}\right)\times$$
$$(r_i + r_m). \qquad (B\text{-}19)$$

Now Equation ( B-14 ) becomes

$$\frac{\partial \nu_j}{\partial \tau} = I_j + \sum_{\substack{i=1 \\ m=j-i}}^{k=j-1} Z_{i,m} \nu_i \nu_m - 2\nu_j \sum_{m=1}^{k} Z_{j,m} \nu_m$$

$$- (1 + A_j \frac{\lambda}{r_j})(\frac{r_j}{r_1})^2 \frac{\partial \nu_j}{\partial \gamma}. \qquad (\text{B-20})$$

At steady state $\partial \nu_j / \partial \tau = 0$ and

$$\frac{d \nu_j}{d \gamma} = \left[ I_j + \sum_{\substack{i=1 \\ m=j-i}}^{k=j-1} Z_{i,m} \nu_i \nu_m - 2\nu_j \sum_{m=1}^{k} Z_{j,m} \nu_m \right] \Bigg/$$

$$(1 + A_j \frac{\lambda}{r_j})(\frac{r_j}{r_1})^2. \qquad (\text{B-21})$$

However ( see Equation ( III-6 )

$$(1 + A_j \frac{\lambda}{r_j})(\frac{r_j}{r_1})^2 = \left[ 1 + A_j \frac{\lambda}{r_1} (\frac{1}{j})^{1/3} \right] j^{2/3}$$

$$(\text{B-22})$$

where (see Equation ( III-49 ))

$$A_j = 1.257 + .400e^{-1.10r_j/\lambda}. \qquad ( B\text{-}23 )$$

Multiplication of the exponential term in Equation ( B-23 ) by $r_1/r_1$ gives  see Equation ( III-6 )

$$A_j = 1.257 + .400e^{-1.10 \left( \frac{r_1}{r_1} \frac{r_j}{\lambda} \right)}$$

$$= 1.257 + .400e^{-1.10j^{1/3}r_1/\lambda}. \qquad ( B\text{-}24 )$$

Substitution of Equation ( B-24 ) into Equation ( B-22 ) gives

$$( 1 + A_j \frac{\lambda}{r_j} )( \frac{r_1}{r_1} )^2 = j^{2/3} + 1.257(\lambda/r_1)j^{1/3} +$$

$$.400(\lambda/r_1)j^{1/3}e^{-1.10j^{1/3}r_1/\lambda}. \qquad ( B\text{-}25 )$$

Substitution of Equation ( B-25 ) into Equation ( B-21 ) gives

$$\frac{d\nu_j}{d\gamma} = \left[ I_j + \sum_{\substack{i=1 \\ m=j-i}}^{k=j-1} Z_{i,m}\nu_i\nu_m - 2\nu_j \sum_{m=1}^{k} Z_{j,m}\nu_m \right] \Bigg/ \qquad ( B\text{-}26 )$$

$$\left[ j^{2/3} + 1.257(\lambda/r_1)j^{1/3} + .400(\lambda/r_1)j^{1/3}e^{-1.10j^{1/3}r_1/\lambda} \right].$$

It should be noted that the parameter $\lambda/r_1$ specifies the particle size range.

APPENDIX C

EVALUATION OF $Z_{i,m}$ , THE DIMENSIONLESS COAGULATION COEFFICIENT

The dimensionless coagulation coefficient is given as (see Equation ( B-19 ))

$$Z_{i,m} = ( \frac{1}{r_i} + A_i \frac{\lambda}{r_i^2} + \frac{1}{r_m} + A_m \frac{\lambda}{r_m^2} )( r_i + r_m ). \qquad ( C-1 )$$

Substitution of Equation ( III-49 ) for the values of $A_i$ and $A_m$ in Equation ( C-1 ) gives

$$Z_{i,m} = \left[ \frac{1}{r_i} + \frac{\lambda}{r_i^2} ( 1.257 + .400e^{-1.10r_i/\lambda} ) + \right.$$

$$\left. \frac{1}{r_m} + \frac{\lambda}{r_m^2} ( 1.257 + .400e^{-1.10r_m/\lambda} ) \right]( r_i + r_m ). \qquad ( C-2 )$$

Multiplication of Equation ( C-2 ) by $r_1/r_1$ produces

$$Z_{i,m} = \left\{ \frac{1}{\left[ \frac{r_i}{r_1} \right]} + \frac{\frac{\lambda}{r_1}}{\left[ \frac{r_i}{r_1} \right]^2} \left( 1.257 + .400e^{-1.10 \frac{r_i}{\lambda} \frac{r_1}{r_1}} \right) + \right.$$

$$\frac{1}{\left[\dfrac{r_m}{r_1}\right]} + \frac{\dfrac{\lambda}{r_1}}{\left[\dfrac{r_m}{r_1}\right]^2}\left(1.257 + .400e^{-1.10\frac{r_m}{\lambda}\frac{r_1}{r_1}}\right)\left(\frac{r_i}{r_1} + \frac{r_m}{r_1}\right).$$

$$( \text{C-3} )$$

But $\dfrac{r_i}{r_1} = i^{1/3}$ and $\dfrac{r_m}{r_1} = m^{1/3}$ ( see Equation ( III-6))

so Equation ( C-3 ) becomes

$$Z_{i,m} = \left(i^{1/3} + m^{1/3}\right)\left[\frac{i^{1/3} + \dfrac{\lambda}{r_1}\left(1.257 + .400e^{-1.10i^{1/3}r_1/\lambda}\right)}{i^{2/3}}\right.$$

$$\left. + \frac{m^{1/3} + \dfrac{\lambda}{r_1}\left(1.257 + .400e^{-1.10m^{1/3}r_1/\lambda}\right)}{m^{2/3}}\right]$$

$$( \text{C-4} )$$

where, for this work, $\lambda/r_1$ takes on the values 0.10, 1.00, and 10.0.

# APPENDIX D

## PROGRAMMING TECHNIQUE FOR THE DIMENSIONLESS COAGULATION COEFFICIENTS

For a system of 400 particles the gain term array for $Z_{i,m}$ (see Table 4) demanded $Z_{i,m}$ coefficients on a diagonal of the array (as shown by the arrow for $j = 5$) for each particle "type". A larger view showed that the gain terms included for all particle "types" required the upper left triangle of the array (see Figure 20).

Much time was wasted attempting to take advantage of the fact that $Z_{i,m}$ equaled $Z_{m,i}$ (see Equation ( IV-2 )) by employing standard symmetric matrix equations to transform the $Z_{i,m}$ symmetric 2-dimensional matrix into a 1-dimensional array. This would be advantageous because only half the array would need to be calculated. The transform was discarded because even 80,000 numbers plus the program and loss coefficients was too large for machine core. An even greater problem was caused because the numbers were not placed in a manageable order; i.e., the numbers on a diagonal of the array were arranged such that access from the main program was too complex.

It was found that the core of the IBM-370/145 was capable of storing a total of 80,000 gain or loss coefficients plus the program. The most logical way to integrate Equation ( IV-3 ) was to employ continuously incremented do-loops. This meant that an equation was needed to reduce the total number of coagulation coefficients necessary to solve Equation ( IV-3 ) from

( 4 X 80,000 for gain + 4 X 160,000 for loss ) = 960,000 numbers

to, at most, 80,000. The factor of four appeared because the integration was fourth-order.

m

|   | 1 | 2 | 3 | 4 | ............... 400 |
|---|---|---|---|---|---|
| 1 | $Z_{1,1}$ | $Z_{1,2}$ | $Z_{1,3}$ | $Z_{1,4}$ | ............... $Z_{1,400}$ |
| 2 | $Z_{2,1}$ | $Z_{2,2}$ | $Z_{2,3}$ | $Z_{2,4}$ | ............... $Z_{2,400}$ |
| 3 | $Z_{3,1}$ | $Z_{3,2}$ | $Z_{3,3}$ | $Z_{3,4}$ | ............... $Z_{3,400}$ |
| 4 | $Z_{4,1}$ | $Z_{4,2}$ | $Z_{4,3}$ | $Z_{4,4}$ | ............... $Z_{4,400}$ |
| 5 | $Z_{5,1}$ | $Z_{5,2}$ | $Z_{5,3}$ | $Z_{5,4}$ | ............... $Z_{5,400}$ |
| 400 | $Z_{400,1}$ | $Z_{400,2}$ | $Z_{400,3}$ | $Z_{400,4}$ | |

i

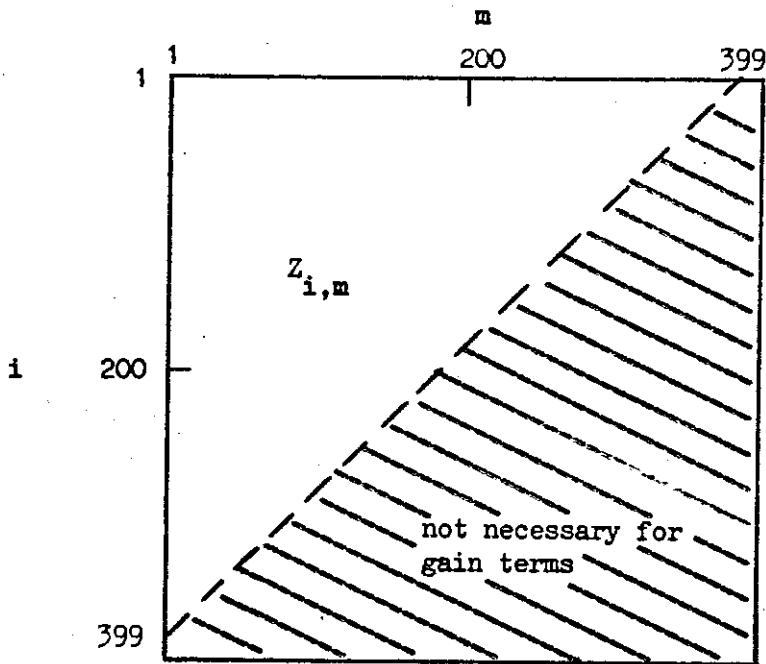Table 4. Gain Term Array for $Z_{i,m}$

Figure 20. $Z_{i,m}$ Gain Term Coefficients Necessary for Solution of
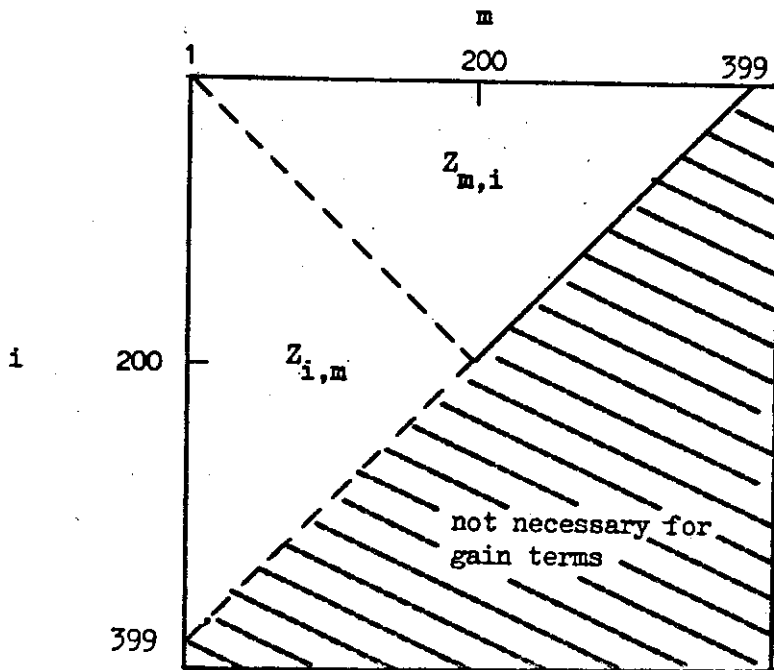Coagulation Equation



Figure 21. Visualization of Left $Z_{i,m}$ Triangle
Transformed into 1-Dimensional Array

Examination of smaller systems and knowledge of the symmetry feat-
ures of this system allowed an equation that would convert the left
triangle of the gain term $Z_{i,m}$ matrix into a logical 1-dimensional
array (see Figure 21). This equation was determined to be

$$IR = 400(m-1) - (m-1)^2 + i - m + 1 \qquad (D-1)$$

where

$$m = i = \text{subscripts of } Z_{i,m} \text{ term}$$
and
$$IR = \text{coefficient of 1-dimensional array}$$

Reversal of the $Z_{i,m}$ subscripts in Equation ( D-1 ) described the
upper triangle of the $Z_{i,m}$ matrix. Thus, Equation ( D-1 ) was used to
describe the entire upper left triangle necessary for the $Z_{i,m}$ gain
terms with only one-fourth of the matrix necessarily calculated.

Examination of the loss term coefficient, $Z_{j,m}$, was now necessary.
It was seen (see Equation ( IV-4 )) that the $Z_{j,m}$ terms would be drawn
in sequence across the matrix (see Table 5 for $j = 5$ ). Various attempts
were made to decrease the number of calculations necessary to describe
the loss term coefficients matrix; however, all attempts failed.

It was necessary to keep in mind that the matrices $Z_{i,m}$ and $Z_{j,m}$
were, in actuality, the same matrix. They were, however, used independent-
ly in the computer program and had to be treated as two separate entities.

Since all attempts to decrease the number of loss term coefficients
failed, a compromise was made. The entire loss term coefficient matrix,
$Z_{j,m}$, was calculated and written on tape in blocks of 8000 numbers. This
was the maximum allowable computer blocksize. The main program was written
to manipulate the entrance and exit of the loss term coefficients in
blocks of 8000 numbers.

The gain term coefficient's 40,000 numbers were also written on tape,
but they were placed after the loss term coefficients. In this manner

m

|  | 1 | 2 | 3 | 4 | | 400 |
|---|---|---|---|---|---|---|
| 1 | $Z_{1,1}$ | $Z_{1,2}$ | $Z_{1,3}$ | $Z_{1,4}$ | $\cdots\cdots\cdots\cdots$ | $Z_{1,400}$ |
| 2 | $Z_{2,1}$ | $Z_{2,2}$ | $Z_{2,3}$ | $Z_{2,4}$ | $\cdots\cdots\cdots\cdots$ | $Z_{2,400}$ |
| 3 | $Z_{3,1}$ | $Z_{3,2}$ | $Z_{3,3}$ | $Z_{3,4}$ | $\cdots\cdots\cdots\cdots$ | $Z_{3,400}$ |
| 4 | $Z_{4,1}$ | $Z_{4,2}$ | $Z_{4,3}$ | $Z_{4,4}$ | $\cdots\cdots\cdots\cdots$ | $Z_{4,400}$ |
| 5 | $Z_{5,1}$ | $Z_{5,2}$ | $Z_{5,3}$ | $Z_{5,4}$ | $\cdots\cdots\cdots\cdots$ | $Z_{5,400}$ |
| $\cdot$ | $\cdot$ | $\cdot$ | $\cdot$ | $\cdot$ | | |
| $\cdot$ | $\cdot$ | $\cdot$ | $\cdot$ | $\cdot$ | | |
| $\cdot$ | $\cdot$ | $\cdot$ | $\cdot$ | $\cdot$ | | |
| $\cdot$ | $\cdot$ | $\cdot$ | $\cdot$ | $\cdot$ | | |
| $\cdot$ | $\cdot$ | $\cdot$ | $\cdot$ | $\cdot$ | | |
| $\cdot$ | $\cdot$ | $\cdot$ | $\cdot$ | $\cdot$ | | |
| $\cdot$ | $\cdot$ | $\cdot$ | $\cdot$ | $\cdot$ | | |
| $\cdot$ | $\cdot$ | $\cdot$ | $\cdot$ | $\cdot$ | | |
| 400 | $Z_{400,1}$ | $Z_{400,2}$ | $Z_{400,3}$ | $Z_{400,4}$ | | |

j

Table 5. Loss Term Array for $Z_{j,m}$

the main program cycled through the tape to the gain term coefficients
which were read into permanent machine core. The tape would then rewind
to the start of the loss term coefficients and the main program would
read the first block of 8000 numbers into core. When the next 8000
numbers were needed, the next block was read into core replacing the
previous one. When the main program had read all 160,000 loss term
coefficients the tape would rewind and restart the cycle. This method
never allowed more than 48,000 numbers to be in core at any time.

A tape was made for $\lambda/r_1 = 1.00$ in the $Z_{i,m}$, $Z_{j,m}$ calculations (see
Equation ( IV-2 )). A sample program used to create the tape can be
found in Appendix E. For work involving the self-preserving size
distribution, two additional tapes were made carrying the values $\lambda/r_1 =$
10.0 and 0.10.

APPENDIX E

PROGRAM USED TO CREATE TAPES FOR DIMENSIONLESS COAGULATION COEFFICIENTS

```
      DIMENSION Z(400,20),C(40000),BB(8000)
101   FORMAT(' ',10X,I3)
      M=0
      MM=0
      KMAX=400
      AB=10.0
      RZ=1./3.
      RX=2./3.
      J=1
C
C     CALCULATION OF LOSS TERM COEFFICIENTS
C
      DO 23 I=1,KMAX
      A=I
      B=J
      ANZO=1.257+.4*EXP((-1.1*(A**RZ))/AB)
      BNZO=1.257+.4*EXP((-1.1*(B**RZ))/AB)
      SNOB=(A**RZ)+(B**RZ)
      SKIN=ANZO*AB
      SKUN=BNZO*AB
      SNOOT=SKIN+A**RZ
      SNEET=SKUN+B**RZ
      J=J-20*M
      Z(I,J)=SNOB*((SNOOT/A**RX)+(SNEET/B**RX))
      J=J+20*M
23    CONTINUE
      J=J+1
      ML=M*20+21
```

Fortran code pages 97 and 98 available from author.

# APPENDIX F

## PROGRAM USED TO DUPLICATE HIDY'S SOLUTION

```
      DIMENSION X(400),XX(400),A(400),Q(400),D(400),F(400),T(400),K(4,40
     10),B(1),C(40000),Z(400,20),BB(8000),ZX(100,1),ZZ(100,1)IK(100,1),
     2IY(100,1)
      REAL K
      READ(5,101)TMAX,KMAX,B(1)
  239 FORMAT(' ','TIME INCREMENT=',3X,F11.6///)
  240 FORMAT(' ',10(2X,E10.3))
  241 FORMAT(' ',15X,'*****************************************')
  242 FORMAT(8(E10.3))
  101 FORMAT(F7.3,I3,F7.3)
  102 FORMAT(' ',10X,I3)
  107 FORMAT(' ','THE TOTAL MASS OF THE SYSTEM=',2X,F7.3)
      L=1
      T(1)=0.0
C
C     CALCULATION OF DIMENSIONLESS TIME INCREMENT
C
      DO 31 N=2,KMAX
      T(N)=T(N-1)+B(L)
   31 CONTINUE
C
C     INITITIALIZATION OF RELATIVE PARTICLE CONCENTRATIONS TO ZERO
C
      DO 92 N=1,KMAX
      X(N)=0.0
      XX(N)=0.0
   92 CONTINUE
C
C     PRINTOUT OF INITIAL CONDITIONS
C
      WRITE(6,239)T(1)
      WRITE(6,240)(X(MM),MM=1,KMAX)
```

## PROGRAM FOR THE STEADY STATE SOLUTION

```
      DIMENSION X(400),XX(400),A(400),Q(400),D(400),F(400),T(400),K(4,400),
     1B(1),C(40000),Z(400,20),BB(8000),ZX(400,1),ZZ(400,1),IK(400,1),IY(400
     2,1),XI(400),G(400)
      REAL K
      READ(5,101)TMAX,KMAX,B(1),AB,BAB
  239 FORMAT(' ','THE DIMENSIONLESS DISTANCE INCREMENT=',3X,F11.6/)
  240 FORMAT(' ',10(2X,E10.3))
  241 FORMAT(' ',15X,'******************************************')
  242 FORMAT(8(E10.3))
  101 FORMAT(F7.3,I3,F7.3,F7.3,F8.5)
  107 FORMAT(' ','THE TOTAL MASS OF THE SYSTEM =',2X,F7.4///)
  102 FORMAT(' ',10X,I3)
      L=1
      T(1)=0.0
C
C     CALCULATION OF THE DIMENSIONLESS DISTANCE INCREMENT
C
      DO 31 N=2,KMAX
      T(N)=T(N-1)+B(L)
   31 CONTINUE
C
C     INITIALIZATION OF RELATIVE PARTICLE CONCENTRATIONS TO ZERO
C
      DO 92 N=1,KMAX
      X(N)=0.0
      XX(N)=0.0
   92 CONTINUE
C
C     CALCULATION OF SETTLING TERMS
C
      CALL SET(KMAX,G,AB)
      N=1
      J=1
```

Fortran code pages 106-111 available from author

## PROGRAM NOMENCLATURE

$X = \nu$

$T = \gamma$

TMAX = dimensionless distance limit

KMAX = number of particles in the system = 400

B = integration increment

AB = value of $\lambda/r_1$

BAB = value of $r_1$

XX = conditions from previous increment needed for Runge-Kutta integration routine

G = settling terms

C = gain term probabilities

XNOT=XNUT = test terms for machine underflow

A = gain to size class summation

Z = loss term probabilities

Q = intermediate loss from size class summation

D = final loss from size class summation

XI = feed to system

F = sum of feed and gains and losses to size classes with division by settling terms

K = Runge-Kutta slope

E = dimensionless mass

$ZX = \eta$

$ZZ = \psi$

The subroutine RPPLOT is a 396 statement plotting routine available in the CSU computer library.

# APPENDIX H

## THE DIMENSIONLESS MASS DERIVATION

For a unit volume of the atmosphere, the mass of particles contained therin is

$$M = \sum_j \frac{4}{3} \pi r_j^3 \rho \, n_j \quad . \qquad ( \text{H-1} )$$

The total mass fraction, $W$, of particles is

$$W = \frac{M}{N} = \sum_j \frac{4}{3} \pi r_j^3 \rho \, \frac{n_j}{N} \quad , \qquad ( \text{H-2} )$$

however, application of the dimensionless concentration (see Equation ( III-57 )) for

$$\frac{n_j}{N} = \nu_j \qquad ( \text{H-3} )$$

and (see Equation ( III-6 ))

$$r_j^3 = r_1^3 \, j \qquad ( \text{H-4} )$$

gives

$$W = \sum_j \frac{4}{3} \pi r_1^3 \, j \, \rho \, \nu_j \quad . \qquad ( \text{H-5} )$$

For programming purposes, the constants contained in Equation ( H-5 ), namely, $4 \pi r_1^3 \rho /3$, are neglected and the dimensionless mass used by Hidy ( 7 ) becomes

$$E = \sum_j \nu_j j \qquad\qquad ( \text{H-6} )$$

For this work the dimensionless mass according to Equation ( H-6 ) was found to remain constant at $E = 1.00$ to $\tau = 1.00$. Hidy ( 7 ) found that about 9% of the material initially present was lost during each integration step. This difference could be due to the difference in integration routines and trapping procedures.

APPENDIX J

CONVERSION OF DIMENSIONLESS CONCENTRATION DISTRIBUTIONS TO SELF-PRESERVING FORM

For the continuous spectrum, the distribution function $n(v,t)$ is defined by the relation

$$dN = n \, dv \qquad (J-1)$$

where dN represents the number of particles per unit volume of fluid in the size range $v + dv$. In the similarity theory proposed by Swift and Friedlander ( 16 ), $n(v,t)$ can be written as

$$n(v,t) = \frac{N^2}{\phi} \, \psi(\eta_v) \qquad (J-2)$$

where $\phi$, the total volume fraction of particles is

$$\phi = \int_0^\infty n \, v \, dv = \text{const.} \qquad (J-3)$$

and

$$\eta_v = \frac{v \, N}{\phi} \, . \qquad (J-4)$$

The function $\psi(\eta_v)$ is independent of time. It represents a particular solution to the coagulation equation written in terms of $n(v,t)$ when sedimentation is not considered. For this work, it is also assumed

that $\psi(\eta_v)$ represents a solution of the coagulation equation for each value of $\gamma$ when sedimentation is not ignored.

Over some ranges of $\gamma$, solutions to the set of equations for the discrete spectrum should display a form analogous to Equation ( J-2 ). It is logical to assume that Equation ( J-4 ) is the proper dimensionless volume for the discrete case, or

$$\eta_{v_j} = \frac{v_j N}{\phi} = \frac{j v_1 N}{\phi} \qquad ( J\text{-}5 )$$

where

$$\phi = \sum_s v_s n_s . \qquad ( J\text{-}6 )$$

To derive the form of the similarity function $\psi$ for the discrete spectrum, it is noted that Equation ( J-1 ) is approximately

$$\Delta N \approx n \, \Delta v \qquad ( J\text{-}7 )$$

Since $\Delta v = v_1$ and $\Delta N = n_j$,

$$n \approx \frac{n_j}{v_1} . \qquad ( J\text{-}8 )$$

When this relation is substituted into Equation ( J-2 ), the proper form of $\psi$ for the discrete distribution is obtained:

$$\psi(\eta_{v_j}) = \frac{n_j \phi}{N^2 v_1} . \qquad ( J\text{-}9 )$$

It is noted that Equations ( J-2 ) and ( J-4 ) are written in terms of volume. An analogous set of equations written in terms of radius are ( 2 )

$$\psi(\,\eta_r\,) = \frac{n\,(\,r,t)\,\phi^{1/3}}{N^{4/3}} \qquad (\,J\text{-}10\,)$$

where

$$\eta_r = r\,\left(\frac{N}{\phi}\right)^{1/3}. \qquad (\,J\text{-}11\,)$$

For the discrete spectrum, the logical forms of Equations ( J-10 ) and ( J-11 ) are

$$\psi(\,\eta_{r_j}\,) = \frac{n_j\,\phi^{1/3}}{\Delta r_j\,N^{4/3}} \qquad (\,J\text{-}12\,)$$

and

$$\eta_{r_j} = r_j\,\left(\frac{N}{\phi}\right)^{1/3} \qquad (\,J\text{-}13\,)$$

where $\phi$ is calculated by

$$\phi = \sum_s (4/3)\,\pi r_s^3 n_s. \qquad (\,J\text{-}14\,)$$

$\psi(\,\eta_{v_j}\,)$ and $\psi(\,\eta_{r_j}\,)$ are related by Equations ( J-9 ) and ( J-12 ) or

$$\frac{\psi(\,^{\eta}r_j\,)}{\psi(\,^{\eta}v_j\,)} = \frac{n_j\,\phi^{1/3}}{\Delta r_j\,N^{4/3}} \quad \frac{N^2\,v_1}{n_j\,\phi}$$

$$= \frac{N^{2/3}\,v_1}{\Delta r_j\,\phi^{2/3}} \cdot \qquad\qquad (\text{ J-15 })$$

Multiplication of Equation ( J-15 ) by $j^{2/3}/j^{2/3}$ and application of Equation ( J-5 ) gives

$$\frac{\psi(\,^{\eta}r_j\,)}{\psi(\,^{\eta}v_j\,)} = \frac{(\,^{\eta}v_j\,)^{2/3}\,v_1^{1/3}}{\Delta r_j\,j^{2/3}} \cdot \qquad\qquad (\text{ J-16 })$$

However, $v_1^{1/3}$ can be represented as

$$v_1^{1/3} = \frac{(36\pi)^{1/3}\,r_1}{3} \cdot \qquad\qquad (\text{ J-17 })$$

In addition, $\Delta r_j$ in a discrete system is

$$\Delta r_j = r_1\left[\ (j+1)^{1/3} - j^{1/3}\right]. \qquad\qquad (\text{ J-18 })$$

Expansion of $(j+1)^{1/3}$ in a Taylor's series with retention of the first term yields

$$\Delta r_j = \frac{r_1\,j^{-2/3}}{3} \cdot \qquad\qquad (\text{ J-19 })$$

Substitution of Equations ( J-17 ) and ( J-18 ) into Equation ( J-16 ) yields a final form of

$$\psi(\,^{\eta}r_j) = \eta_{v_j}^{2/3}\,(36\pi)^{1/3}\,\psi(\,^{\eta}v_j)\,.\qquad(\text{J-20})$$

Relations also exist between $\eta_{r_j}$ and $\eta_{v_j}$. Application of Equations ( J-13 ) and ( J-5 ) gives

$$\frac{\eta_{r_j}}{\eta_{v_j}^{1/3}} = \frac{r_j\,N^{1/3}}{\phi^{1/3}}\ \frac{\phi^{1/3}}{j^{1/3}\,v_1^{1/3}N^{1/3}}$$

$$= \frac{r_j}{j^{1/3}\,v_1^{1/3}}\,.\qquad(\text{J-21})$$

However,

$$v_1^{1/3} = (\frac{4\pi r_1^3}{3})^{1/3}\,.\qquad(\text{J-22})$$

Substitution of Equation ( J-22 ) into Equation ( J-21 ) with $r_j = r_1\,j^{1/3}$ (see Equation ( III-6)) gives

$$\eta_{r_j} = (\frac{3}{4\pi})^{1/3}\,\eta_{v_j}^{1/3}\,.\qquad(\text{J-23})$$

The continuous coordinates $\psi(\,^{\eta}r)$ and $\eta_r$ are to be simulated by the coordinates $\psi(\,^{\eta}r_j)$ and $\eta_{r_j}$ for the discrete case. $\psi$ and $\eta$ for the discrete case can be transformed into coordinates containing $\nu$ and $j$ by the proper substitutions. Rewriting Equation ( J-12 ) gives

$$\psi(\,^{\eta}r_j) = \frac{\dfrac{n_j}{N}\left[\displaystyle\sum_s \frac{4\pi r_s^3}{3}\frac{n_s}{N}\right]^{1/3}}{\Delta r_j}\,.\qquad(\text{J-24})$$

By using the dimensionless particle concentration, Equation ( J-24 ) becomes

$$\psi(\,{}^{\eta}r_j\,) = \frac{\nu_j\left[\displaystyle\sum \frac{4\pi r_s^3 \nu_s}{3}\right]^{1/3}}{\Delta r_j}\,. \qquad (\text{ J-25 })$$

Application of Equation ( J-19 ) for $\Delta r_j$ and recognition that $r_s^3 = r_1^3 s$ gives

$$\psi(\,{}^{\eta}r_j\,) = 3\,j^{2/3}\nu_j\left[\sum_s \frac{4\pi s\,\nu_s}{3}\right]^{1/3} \qquad (\text{ J-26 })$$

In a discrete system, the approximation of $\Delta r_j = [(\,j+1\,)^{1/3} - j^{1/3}]$ by $r_1\,j^{-2/3}/3$ is very good for $j>10$. The error in using the approximation averages less than 4% for $j<10$. For $j>50$ the error is less than 1%.

The coordinate ${}^{\eta}r_j$ is defined by Equation ( J-13 ) and using the definition for $\phi$ yields

$$ {}^{\eta}r_j = \frac{r_j}{\left[\displaystyle\sum_s \frac{4\pi r_s^3}{3}\frac{n_s}{N}\right]^{1/3}} \qquad (\text{ J-27 })$$

Using the dimensionless particle concentration and substitution of $r_j = r_1\,j^{1/3}$ provides

$$ {}^{\eta}r_j = \frac{j^{1/3}}{\left[\displaystyle\sum_s \frac{4\pi s\,\nu_s}{3}\right]^{1/3}}\,. \qquad (\text{ J-28 })$$

APPENDIX K

PROGRAM FOR THE CALCULATION OF THE SELF-PRESERVING SIZE DISTRIBUTION

```
      DIMENSION X(1200),ZZ(1200,1),ZX(1200,1),IK(1200,1),IY(1200,1)
242   FORMAT(8(E10.3))
240   FORMAT(' ',10(2X,E10.3))
244   FORMAT(' ',20X,'DIMENSIONLESS PLOT IN TERMS OF RADIUS')
245   FORMAT(' ',20X,'DIMENSIONLESS PLOT IN TERMS OF VOLUME')
      READ(5,242)(X(I),I=1,1200)
      ZAB=0.0
      JAB=1
      DO 3 I=1,400
      S=I*JAB
      ZAB=ZAB+S*X(I)*(4./3.)*3.14
3     CONTINUE
      JAB=1000
      DO 4 I=401,800
      J=I-400
      S=J*JAB
      ZAB=ZAB+S*X(I)*(4./3.)*3.14
4     CONTINUE
      JAB=1000000
      DO 5 I=801,1200
      J=I-800
      S=J*JAB
      ZAB=ZAB+S*X(I)*(4./3.)*3.14
5     CONTINUE
      ZAB=ZAB**(1./3.)
      JAB=1
      DO 6 I=1,400
      S=I*JAB
```

Fortran code pages 122-125 available from author.